JETIR.ORG ISSN: 2349-5162 | ESTD Year : 2014 | Monthly Issue
JOURNAL OF EMERGING TECHNOLOGIES AND INNOVATIVE RESEARCH (JETIR)
An International Scholarly Open Access, Peer-reviewed, Refereed Journal

CHARACTERIZATION OF LOWEST OXYGEN ENVIRONMENTS WITHIN ANCIENT UPWELLING ENVIRONMENTS: A CASE STUDY FROM THE CAMPANIAN-MAASTRICHTIAN AT WEST-CENTRAL SINAI, EGYPT

Orabi H. Orabi[1], Hassan I. Frahat[2], Maha M. Mahmoud[2] and Fares I. Khedr[2]

1- Faculty of Science, Geology Department, Menoufia University, Egypt

2- Faculty of Science, Geology Department, Suez University, Egypt

Abstract

The Late Cretaceous Period was characterized by nutrient-rich conditions driven by intense coastal upwelling. This upwelling system, fueled by strong coastal winds, particularly during the Maastrichtian, elevated nutrient levels in surface waters, as evidenced by geochemical proxies and benthic foraminiferal data. Benthic foraminifera, widely used as indicators of past ocean depths and depositional environments, were studied in the Campanian-Maastrichtian (C-M) marine rocks of the Sudr Formation from the Gabal Nezazzat section (west-central Sinai, Egypt). Nine planktonic foraminiferal zones are recorded through the Nezzazat section, ranging from CF9 to CF1. A total of 71 samples, comprising 69 species across 35 genera, were analyzed to infer species diversity, interrelationships, and changes in palaeo-environmental conditions, palaeo-oxygenation, palaeo-productivity, and palaeo-depth within the C-M successions.

The Campanian deposits were formed in outer neritic to upper bathyal environments (201.6–539.84 m), characterized by low organic matter flux (HOFS: 4.5% to 9%), low total organic carbon (TOC < 3), and well-oxygenated conditions (BFOI: 33.3 to 67.3; oxic >0.3 mL/L O_2). The transition from the Campanian to the Maastrichtian occurred in outer neritic to deeper bathyal settings, maintaining low productivity and well-oxygenated conditions. Early Maastrichtian deposits indicate shallower depositional environments (113.5–479.75 m) with reduced oxygen availability at the seafloor (BFOI: 40–60; dysoxic 0.1–0.3 mL/L O_2), associated with increased organic matter flux and higher TOC values (>4). These conditions deepened through the late Maastrichtian, with upwelling-driven nutrient enrichment persisting throughout the period

Keywords: low-oxygen, Campanian-Maastrichtian, Gebel Nazzazat, Sinai, Benthic foraminiferal.

1. INTRODUCTION

Upwelling is a physical oceanographic phenomenon that significantly influences marine ecosystems, particularly in terms of primary productivity and nutrient dynamics (Wang et al., 2015). The upwelling process involves the movement of cold and nutrient-rich waters from a water depth of a few hundred meters to the surface, thus stimulating biological productivity in the euphotic zone (Aguiar et al., 2014; Cao et al., 2014; Avila-Alonso et al., 2020; Ioannou et al., 2022). Water that rises to the surface due to upwelling is typically colder and is rich in nutrients. These nutrients "fertilize" surface waters, meaning that these surface waters often have high biological productivity. Soudry et al. (2006) demonstrated that the combined effects of global post-Santonian cooling, sea-level high stands, and plate configuration drove the evolution of this upwelling system.

Benthic foraminifera are widely used as indicators for inferring paleodepths as they exist and are found from the ocean floor (the shelf) to the abyssal area. Data on the depth distribution of fossil benthic foraminifera is typically gathered from standard marine environments, including those formed under upwelling conditions. The primary factors that drive changes in the composition of benthic foraminiferal assemblages are high food fluxes and oxygen depletion at the seafloor, which can mask the paleobathymetric signal (Avnaim-Katav et al., 2015; Ashckenazi-Polivoda et al., 2018). Consequently, they are one of the most commonly used faunal indicators for environmental and sea-level changes and are generally used to infer paleodepth (shelf, slope bathyal, or abyssal depths) (Leckie and Olson, 2003). Salinity, temperature, substrate type, and water depth are less important. While oxygen concentration becomes the primary limiting factor on the sea floor, food is abundant in high-productivity conditions (Jorissen et al., 1995; van der Zwaan et al., 1999; Ernst and van der Zwaan, 2004).

The Late Cretaceous Period (100.5–66.04 million years ago) is distinguished by a "hothouse" climate (Huber et al., 2002; Miller et al., 2020), which featured elevated atmospheric CO2 concentrations (O'Brien et al., 2017) and notably high global sea levels (Miller et al., 2005; Haq, 2014). The Campanian–Maastrichtian (~83–66 million years ago) marked a period of global climate cooling, which occurred during the Late Campanian Event (LCE) and the Campanian–Maastrichtian Transition Event (CMTE) [Huber et al.,2018), accompanied by Alterations in the global ocean circulation, particularly in the high southern latitudes (Donnadieu et al.,2016). Numerous rock types make up this succession during the Late Cretaceous, including chert, phosphorite, marl, organic-rich carbonate, and chalk. *Buliminina* has been associated with low oxygen levels and high organic productivity (Sen Gupta and Machain-Castillo, 1993; Ashckenazi-Polivoda et al., 2010; Farouk et al., 2023; Trubin et al., 2023). It is possible to recreate changing low-oxygen paleoenvironments by using their existence in foraminiferal assemblages.

This paper provides a detailed paleobathymetric reconstruction of Campanian-Maastrichtian at West-Central Sinai based on the changes in benthic assemblages comprising 69 species belonging to 35 genera. Specifically, this study demonstrates that depth distribution models based on known cosmopolitan Late

Cretaceous benthic foraminifera species in normal marine settings are also applicable as proxies for paleobathymetry in high productivity regimes, as well as to track oxygen stress in bottom-and-pore waters at the time of deposition.

2. GEOLOGICAL SETTING AND LITHOSTRATIGRAPHY

The area of the present study (Fig. 1) delineated a basin, that developed during the Late Cretaceous Laramid Orogeny, creating the Syrian Arc System (Bartov and Steinitz, 1977; El Shazly, 1977; Youssef, 2003; Saleh et al., 2017) and representing deep basinal depressions (paleodepth: 500-600 m) (Speijer and Van der Zwaan, 1994; El-Ayaat and Khalifa, 2010). During the Coniacian period, the polyphase closure of the Tethys Ocean led to a regressive phase over NE Egypt, where a shallow basin trending NE-SW carries about 200 m of argillaceous sandstone section distinguishes the central part of the Gulf of Suez and extends on both sides. The Coniacian in Egypt is marked by the uplifting of most of the Egyptian Basin (Issawi et al., 2009).

The Santonian global events were marked by folding events followed by rifting episodes. Hence, a reduction in the global tectonic events took place in the Campanian and most of the Maastrichtian. During the late Maastrichtian, the so-called Mediterranean Seuil (Dercourt et al., 1993; Permian, 2013; Issawi et al., 2018) separating western (Atlantic) Tethys from eastern Tethys registered extensional tectonic resulting in a horst and graben mosaic (Camoin et al., 1993; Lüning et al., 2004).

Traditionally, Sinai area is subdivided into two main structure units, the so-called stable shelf also known as the Nile Basin in the south, and the unstable shelf, also known as the Syrian Arc, in the north (Said, 1960; Shahar, 1994 and Tawadros, 2001; Orabi and Zahran, 2014). The Nile Basin experienced little structural deformation during the early Paleogene, whereas the Syrian Arc is characterized by a fold belt that has been tectonically active since the Late Cretaceous (Shahar, 1994).

The Nazzazat section (Fig. 1) is located in the south-western part of Sinai, approximately 60 km south of Abu Zeneima city, with coordinates around Longitude 33°13'–33°17'E and Latitude 28°42'–28°50'N. This geological section has been important in understanding the tectonic evolution of the Sinai Peninsula, especially during the period of tectonic spreading associated with the opening of the Red Sea and the Gulf of Suez.

To date, there has been no consensus on the nomenclature for the fine subdivision of the Senonian rock units in West-Central Sinai and the Gulf of Suez (Fig. 2). The following lithostratigraphic subdivisions of the Senonian rock groups are suggested from base to top by contrasting the sequence in the studied area with the descriptions provided in southern Egypt (e.g., Youssef, 1957; Said, 1962; Issawi et al., 2009; Lüger, 1985, and Cherif et al., 1989).

2.1 The Duwi Formation (early late Campanian)

This rock unit, known as the phosphate-producing sequence of Qusseir, Safaga, Abu Tartur, and other locations in southern Egypt, was named by Ghorab (1961) and later assigned to the Campanian age by Youssef (1957) and Said (1962). In the southern part of the Western Desert, Klitsch (1978) and Lüger (1985) suggested that the Duwi Formation spans the late Campanian to early Maastrichtian age. In the studied area, this sequence consists of marls, calcareous sandstones, shales, and carbonates, with chert bands. The most prominent mega-invertebrate in this unit is *Pychnodonta vesicularis*, which is mainly found in the upper part of the sequence and is considered an indicator of the Campanian in Egypt (Abbass, 1962).

Ott d'Estevou et al. (1986) observed that above a sequence containing phosphatic beds and banks of *Pychnodonta vesicularis* (likely equivalent to the Duwi Formation in this study), the Maastrichtian begins with chalky beds that are devoid of *P. vesicularis*. The thickness of this formation reaches 7 meters in Gebel Nazzazat (Fig. 2).

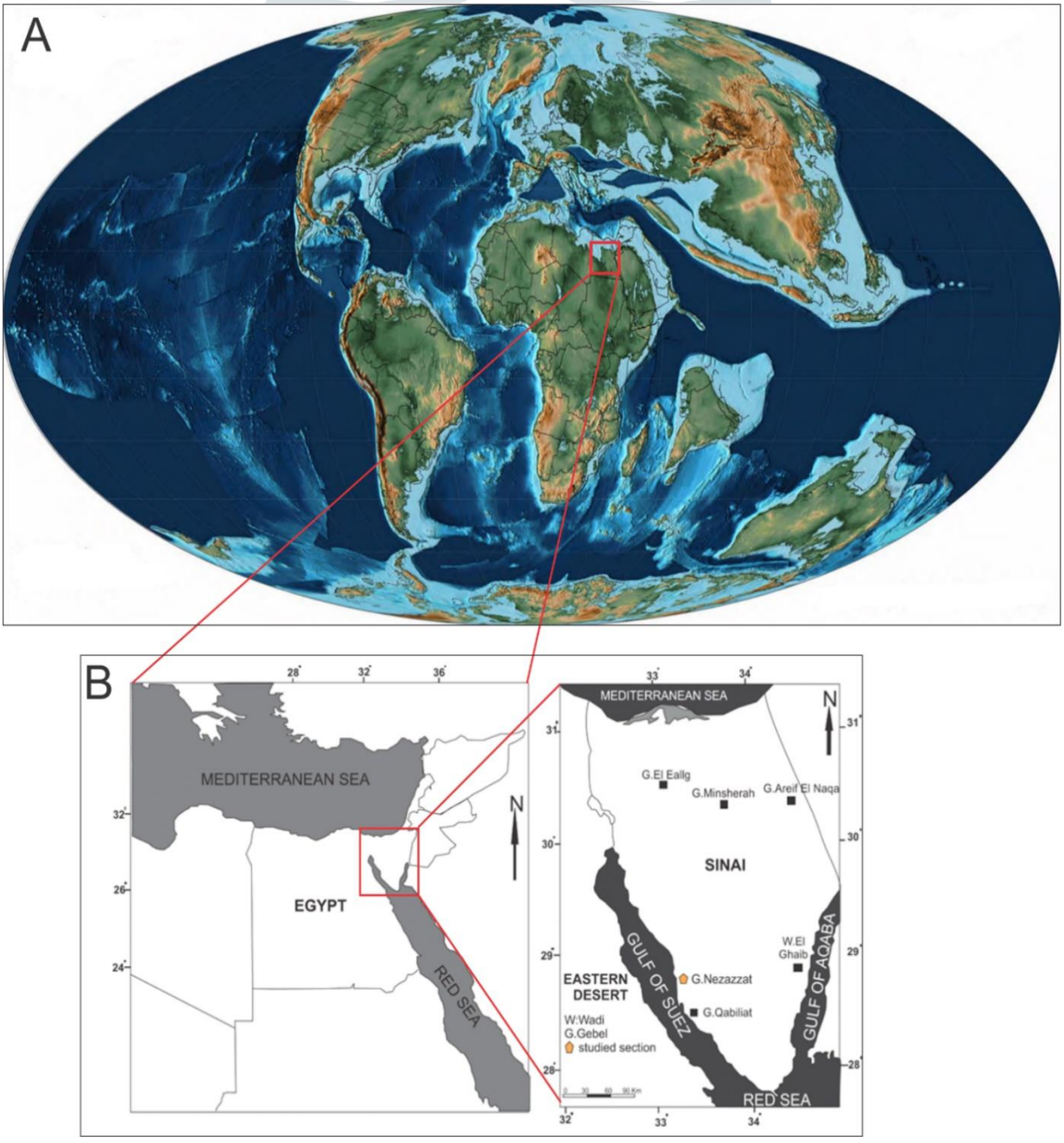


Fig. 1. (A) Paleogeographical locality of Egypt during Maastrichtian time (modified after Scotese, 2014); (B) Location map of the study area of Gebel Nazzazat, West Central Sinai.

2.2 The Sudr Formation (late Campanian-Maastrichtian)

Ghorab (1961) subdivided the Sudr Formation (Campanian-Maastrichtian) into two members; the lower one is the Markha Chalk Member (late Campanian) is a sequence of chalks of characteristically brown color in the subsurface section of the Gulf of Suez. The upper member or Abu Zeneima Member (Maastrichtian) is very similar to the underlying Markha Member and caped by the Dakhla Formation of the Paleocene age (Fig.2).

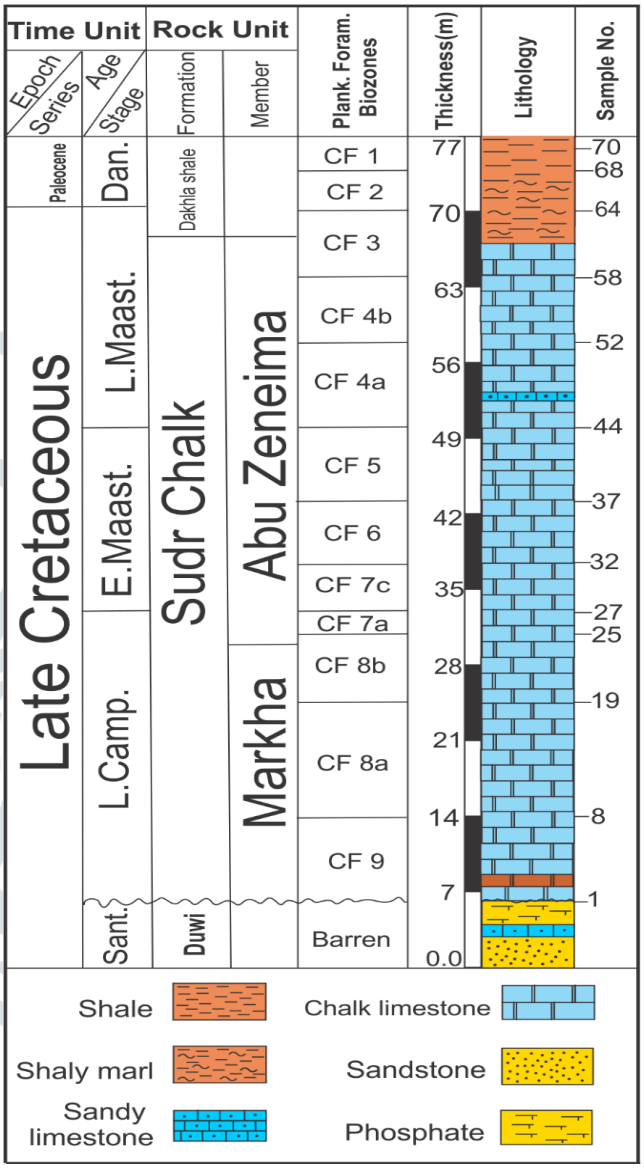


Fig. 2. Measured stratigraphic sections showing the lithostratigraphic units in Gebel Nezazzzat, West Central Sinai.

The Sudr Formation is a chalk sequence that occasionally produces chert nodules or bands. Planktic foraminifera is typically abundant in it, and it transitions to marl or argillaceous limestone with chert bands until descending into the grey shales of the Dakhla Formation. In Gebel Nazzazat, this formation is about 60 meters thick.

2.3 Dakhla Formation (Paleocene)

The Sudr Formation is overlain by the Dakhla Formation (Said, 1961), which alternates between greenish-grey fissile marl and greyish-brown laminated shale with marly limestone intercalations. It attains a thickness of about 10 meters (Fig. 2).

3. MATERIAL AND METHODS

3.1 SAMPLING

A total of 71 samples were collected and dried in an oven at 50°C for a minimum of 24 hours. Approximately 50 g from each sample were immersed in a 10% Hydrogen Peroxide (H_2O_2)solution, followed by washing through 250, 125, and 63 mesh sieves. The samples were then dried and the residue from each sample was examined under a stereomicroscope. The foraminifera tests were carefully selected and placed onto faunal slides. From the more abundant samples, around 250–350 foraminifera specimens were picked from a size fraction of ≥63 μm or more (Douglas, 1973), while approximately 175 specimens were selected from the less abundant samples. (Fatela and Taborda, 2002). The most important and abundant foraminifera are photographed using scanning electron microscopy (JEOL JSM-5500 LV) of Alexandria University (Plates 1-4).

3.2 BENTHIC FORAMINIFERAL ANALYSIS

Based on the foraminifera abundance database, the following parameters were calculated; The Total Foraminifera Number (**TFN**) represents the total count of foraminifera, represents the water depth condition, with an increase in TFN corresponding to a rise in water depth, which includes both planktic and benthic foraminifera, the planktic ratio (**P%**) or the foraminiferal population index of oceans (Gibson, 1989), serves to define various marine environments by assessing the relative abundance of planktic foraminifera. In inner shelf environments (10–50 meters depth), planktic foraminifera are uncommon, with P% below 8%, and species diversity is low. On the middle shelf (50–100 meters depth), P% ranges from 8–25%, indicating a greater abundance of planktic foraminifera and increased species diversity. The outer shelf (100–200 meters depth) generally exhibits a high P% of around 70%, reflecting a greater presence of planktic species. On the middle slope (400–800 meters depth), a very high P% of 90% is observed, demonstrating a dominant occurrence of planktic foraminifera, typical of deeper marine environments (Olsson and Nyong, 1984)is calculated as: $P\%=(P/P+B)\times100$.

The benthic foraminiferal number (**BFN**) is an important indicator for assessing past oxygen levels and organic matter flux (Jorissen et al., 1995). In low-oxygen sediments, the BFN generally declines (Friedrich et al., 2003). Conversely, higher BFN values are found when there is an increased supply of organic matter to the seafloor (Jorissen et al., 1995; Murray, 2000; Friedrich and Hemleben, 2007; Vancoppenolle et al., 2022).

The calcareous/agglutinated foraminifera ratio **(C/A%),** the epifaunal percentage **(Epi%),** Several studies have highlighted a link between the microhabitats of benthic foraminifera and the abundance of epifaunal species (Corliss, 1985; Corliss and Chen, 1988; Jorissen et al., 1995). A greater presence of epifaunal species usually signifies environments with higher oxygen levels and/or lower nutrient concentrations (Bernhard, 1986) and represents the proportion of epifaunal foraminifera, calculated as: $Epi\%=(E/E+I)\times100$.

B/R ratio (= buliminids / (buliminids + rotaliids). The buliminids group includes species such as *Eouvigerina* Cushman, *Bolivinoides* Cushman, *Bolivina* d'Orbigny, *Loxostomum* Ehrenberg, *Praebulimina* Hofker, *Neobulimina* Cushman and Wickenden, and *Siphogenerinoides* Cushman. The rotaliids group includes species like *Alabamina* Toulmin, *Angulogavelinella* Hofker, *Cibicides* de Montfort, *Gavelinella* Brotzen, *Gyroidinoides* Brotzen, and *Osangularia* Brotzen. This ratio is often used to evaluate changes in environmental conditions, such as oxygenation levels or organic matter flux (Ashckenazi et al., 2017).

Additionally, species richness (**S**) and Shannon index (**H**) are used as a proxy for species diversity, **BFOI** (Benthic Foraminifera Oxygen Index (Kaiho 1991; Farouk et al..2024) is calculated as [O/(O+D) × 100], where dysoxic (D), suboxic (S), and Oxic (O). The relative abundances of high organic–flux species (%**HOFS**) are estimated for identification the of nutrient availability. The following species are considered as high–organic–flux species—*Bolivinoides decorata, B. miliaris, B. draco, Bolivina incrassata, Eouvigerina subsculptura, Neoflabellina* spp., *Praebulimina kickapooensis, P. reussi, Pseudonodosaria manifesta, Sitella fabilis, Spiroplectinella* spp. *and Pseudouvigerina plummerae.* (Corliss,1991; Van der Zwaan et al.,1999; Jorissen et al., 2007; Farouk et al..2024)

To estimate paleodepth within the section, two formulas are applied. The first is as follows;

Paleodepth (m) = e^(3.58718 + (0.03534 * %P)),

Where %P is calculated as 100 times the ratio of planktonic foraminifera to the total number of foraminifera, excluding environmental stress taxa. Environmental stress taxa include genera such as Bulimina (excluding costulate forms), Uvigerina, and Valvulineria (Van der Zwaan et al., 1990; Van Hinsbergen et al., 2005; Rahmouna et al., 2022).

The second formula, based on research by De Rijk et al. (1999) on 15 recent Mediterranean transects, is;

Depth (D) = e^((%P + 81.9) / 24),

Where %P is calculated as P / (P + B) * 100 (Shahin., 2022).

Samples from the Campanian-Maastrichtian interval were selected to determine the Total Organic Carbon (TOC) content using a Hochtemperatur-TOC/TNb-Analysator (Liqui TOC). Approximately 200 mg of pulverized sample was used for the analysis. To eliminate carbonate, the samples were treated with 10% aqueous hydrochloric acid. The resulting residue was then used for the TOC determination via combustion analysis at temperatures reaching 850 °C. The evolved CO_2 gas was recorded as a percentage of carbon, and its concentration was measured quantitatively in real time using infrared detectors.

4. RESULTS

4.1. BIOSTRATIGRAPHY

The biostratigraphical distribution of the benthic foraminifera in the examined sections is illustrated in Figure 3. The zonal scheme adopted in this study follows the boundaries established by Caron (1985), Li and Keller (1998a, b), Li et al. (1999), and Arz and Molina (2002) for Cretaceous planktic foraminifera, with some modifications made in the current study to achieve a more refined biostratigraphical resolution.

4.1.1. *Globotruncanella havanensis* Zone (CF9)

The base of this zone isn't defined. We proposed to place the first appearance of planktic foraminifera in the studied sections, i.e. near the top of the Duwi Formation**.**

Benthic Assemblage*:* This zone includes some benthic species *as Praebulimina aspera, P. reussi, P. kickapooensis, Anomalinoides praeacutus, Bolivinoides laevigatus, B. decorates, Gyroidinoides globosus, Angulogavelinella gracilis, Lenticulina midwayensis, Lenticulina* ssp. and *Nodosaria vertebralis* (Fig. 3).

Age: late Campanian.

Thickness: It attains a thickness of 7 m in the Sudr Formation.

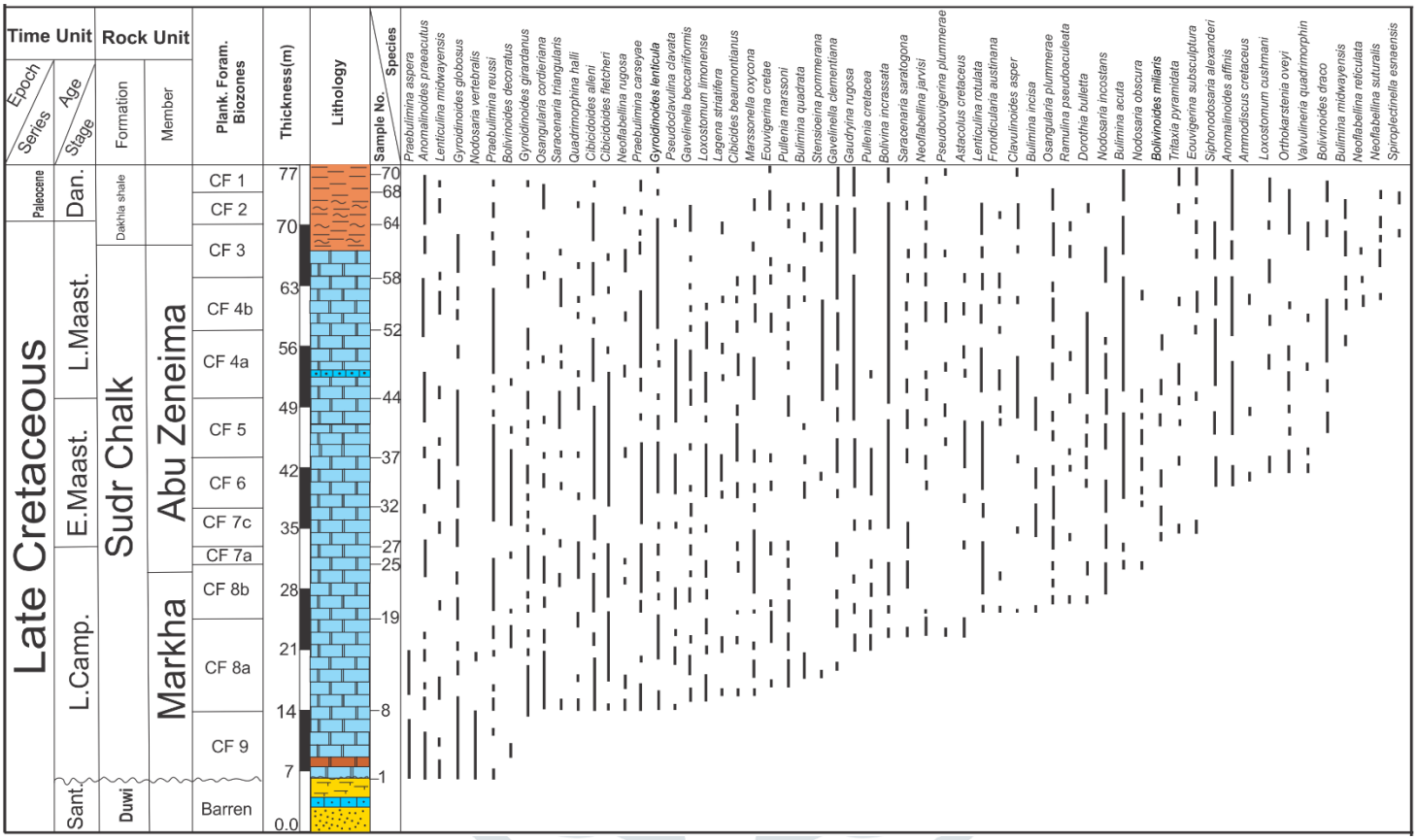


Fig.3. Range charts of the identified Campanian–Maastrichtian benthic foraminifera.

4.1.2. *Globotruncana aegyptiaca* Subzone (CF8a)

The FA of Rugoglobigerina hexacamerata at the top and the FA of the index taxon Globotruncana aegyptiaca at the base recognize this subzone (Li et al., 1999).

Benthic Assemblage: including *Anomalinoides praeacutus, Osangularia cordieriana, Cibicidoides alleni, C. praecursorius, Saracenaria triangularis, S. saratogona, Gyroidinoides tellburmaensis, Bolivinoides decorate, Neoflabellina jarvisi, N. rugosa, Bulimina quadrata, Lenticulina cultrate, Pullenia marssoni, Lagena striatifera, L. hispida, Loxostomum limonense, and Quadrimorphina halli.*

Age: late Campanian.

Thickness: It attains a thickness of 11m in Sudr Formation.

4.1.3. *Rugoglobigerina hexacamerata* Subzone (CF8b)

The FA of Contusotruncana plicata at the top and Rugoglobigerina hexacamerata at the base characterize this subzone. This subzone is Equivalent to the CF8b Subzone of Li et al. (1999).

Benthic Assemblage: some benthic species are recorded, including *Anomalinoides acuta*, *A. praeacutus, Bulimina incisa*, *Gaudryina rugosa*, *Pseudoclavulina clavate, Marssonella oxycona, Guttulina trigonula, Cibicides beaumontianus, C. fletcheri, C. lobatulus, Gyroidinoides girardanus, Osnagularia plummerae,* and *Eouvigerina cretae.* (Fig.3).

Other species that are occasionally common (up to 10%) are *Bolivina incrassata, Bolivinoides decoratus, Praebulimina reussi, Gavelinella clementiana,*

Age: late Campanian.

Thickness: It attains a thickness of 6 m in the Sudr Formation.

4.1.4. *Gansserina gansseri* Zone (CF7)

The *Gansserina gansseri* Zone was divided into three subzones by Saidi and Zaghbib-Turki (2016) to obtain a higher resolution time control: the late Campanian *Rugoglobigerina rotundata* subzone (CF7a), and the two early Maastrichtian *Rugoglobigerina scotti* Subzone (CF7b) and *Planoglobulina acervulinoides* Subzone (CF7c).

This zone is defined by the FA of *Gansserina gansseri* at the base and the FA of *Abathomphalus mayaroensis* at the top. This zone is equal to the CF7 zone of Li and Keller (1998a, b) and Li et al. (1999). In the studied section, this zone is further split into two subzones to provide enhanced resolution for time control (Fig. 3).

4.1.4.1. *Contusotruncana plicata* subzone (CF7a)

This subzone is defined by the FA of *Contusotruncana plicata* at the base and the FA of *Planoglobulina acervulinoides* at the top.

Benthic Assemblage: including *Lenticulina rotulata, Saracenaria saratogona, Cibicidoides pseudoacutus, C. alleni*, *Eouvigerina subsculptura*, Bulimina acuta, *Bolivinoides miliaris*, *Gavelinella beccariiformis, G. vombensis, Bulimina acuta, Gyroidinoides lenticula, Orthokarstenia oveyi* and *Spiroplectinella dentate*.

Age: latest Campanian.

Thickness: It attains a thickness of 2 m at Gebel Nezzazat from the upper part of the Sudr Formation.

4.1.4.2. *Planoglobulina acervulinoides* Subzone (CF7c)

This subzone spans from the first appearance (FA) of *Planoglobulina acervulinoides* to the first appearance (FA) of *Contusotruncana contusa* at the upper boundary.

Several authors note that the first appearance datum (FAD) of *Gansserina gansseri* (Bolli) is associated with the Early Maastrichtian boundary (Robaszynski et al.,1984; Li.,1998a; Li, L., et al 1999; Farouk.,2014; Hewaidy et al., 2017), particularly in the southern Tethys region, including Egypt. However, in other regions, it appears earlier, during the Upper Campanian (Gradstein et al., 2012). In this study, the FAD of *Gansserina gansseri* (Bolli) is used as a marker for the base of the Maastrichtian.

Benthic Assemblage: It resembles the zone beneath

Age: early Maastrichtian**.**

Thickness: It attains about 5m in the Sudr Formation.

4.1.5. *Contusotruncana contusa* Zone (CF6)

The zone is delineated by the first appearance (FA) of *Contusotruncana contusa* at its base and the last appearance (LA) of *Globotruncana linneiana* at its top. This zone corresponds to the CF6 zone established by Li and Keller (1998a,b) and Li et al. (1999).

Benthic Assemblage: It is similar to the underlying zone, except for *Tritaxia pyramidata, Ammodiscus cretaceous, Pseudouvigerina plummerae, Pullenia cretacea, Anomalinoides affinis, Siphonodosaria alexanderi, Saracenaria triangularis, Gavelinella pertusa and Astacolus cretaceous.*

Age: late early Maastrichtian.

Thickness: Covers an interval of 5m in the Sudr Formation.

4.1.6. *Pseudotextularia intermedia* Zone (CF5)

It is defined from the FAD *Racemiguembelina fructicosa* (Egger) found at the top and the LA of the Globotruncana linneiana at the base (Li and Keller 1998a,b, and Li et al. 1999).

Benthic Assemblage: a diverse benthic assemblage is recorded, including *Anomalinoides praeacutus, Bulimina midwayensis, B. incisa, B. quadrata Praebulimina reussi, Gaudryina rugosa, Neoflabellina jarvisi, N. rugosa, N. suturalis Gyroidinoides girardanus, G. subangulatus, G. lenticula, Stensioeina pommerana, Sitella fabilis, Gavelinella beccariiformis, G. clementiana, G. vombensis, Bolivinoides draco, Nodosaria incostans, N. obscura, L. midwayensis, L. rotulata, Ramulina pseudoaculeata, Lagena striatifera, Frondicularia austinana* and *Astacolus cretaceous*.

Age: late early Maastrichtian.

Thickness: Covers an interval of 7m in the Sudr Formation.

4.1.7. *Racemiguembelina fructicosa* Zone (CF4)

To provide a greater resolution time control, this zone is divided into two subzones in the parts under study.

4.1.7.1. *Racemiguembelina fructicosa* Subzone (CF4a)

It can be characterized by the FA of *Racemiguembelina* fructicosa at the base of this subzone to the FA of *Abathomphalus mayaroensis* at the top.

Benthic assemblage: A varied benthic assemblage is observed just like the underlying subzone and others are included as Neoflabellina reticulata, *Loxostomum cushmani, Osnagularia plummerae*. It is characterized by *Spiroplectinella dentate, Spiroplectammina esnaensis* and *Gaudryina pyramidata.*

Age: latest early Maastrichtian.

Thickness: It attains a thickness of 8m in the Sudr Formation.

4.1.7.2. *Abathomphalus mayaroensis* Subzone (CF4b)

The subzone is characterized by the first appearance of *Abathomphalus mayaroensis* at its base and the first appearance of *Pseudoguembelina hariaensis* at its top.

Benthic Assemblage: It resembles the zone beneath.

Age: late Maastrichtian.

Thickness: This zone occupies a thickness of 6m at Gebel Nazzazat.

4.1.8. *Pseudoguembelina hariaensis* Zone (CF3)

The *Pseudoguembelina hariaensis* Zone is delineated by the first appearance of *Pseudoguembelina hariaensis* at its base and the first appearance of *Pseudoguembelina palpebra* at its top (Li and Keller 1998a,b, and Li et al. 1999).

Benthic Assemblage: Although some species disappear from this zone, there are also a lot of species that continue such as *Clavulinoides asper, Gaudryina rugosa, Quadrimorphina halli, Pullenia marssoni, Bulimina acuta, B. midwayensis, B. quadrata, Praebulimina reussi, Eouvigerina create, Cibicides praecursorius, Gyroidinoides lenticula, Neoflabellina rugosa, N. suturalis, Angulogavelinella gracilis and Oolina globulosa.*

Age: late Maastrichtian.

Thickness: This zone occupies a thickness of 6m (4m of the uppermost part of the Sudr and 2m of the basal part of the Dakhla Formation).

4.1.9. *Pseudogumbelina palpebra* Zone (CF2)

This zone is defined by the FA of Plummerita hantkeninoides at the top and the FA of the Pseudoguembelina palpebra at the base and of the biozone.

Benthic Assemblage: It is characterized by *Angulogavelinella abudurbensis, Bolivina incrassata, Lenticulina midwayensis, Neoflabellina suturalis, N. jarvisi, Orthokarstenia oveyi, Marssonella oxycona, Clavulinoides asper, Gaudryina rugosa, Osangularia cordieriana, Eouvigerina subsculptura, E. create, Pseudouvigerina plummerae.* Where the *Cibicidoides* and Lenticulina represented a second major constituent of this biofacies.

Age: late Maastrichtian.

Thickness: Thickness: It attains a thickness of 6m in the Dakhla Formation.

4.1.10. *Plummerita hantkeninoides* Zone (CF1)

The zone is characterized by the total range of the *Plummerita hantkeninoides* (Brönnimann). This zone corresponds to the CF1 zone established by Li et al. (1999).

Benthic Assemblage: *Angulogavelinella gracilis, Gyroidinoides lenticula, Anomalinoides praeacutus, Osangularia plummere, Cibicidoides lobatus, C. praecursorius, Lenticulina cultrate, Bolivina incrassata gigantea, Tritaxia pyramidata, Clavulinoides asper, Ammodiscus cretaceous,* and *Spiroplectinella dentate*.

Age: latest Maastrichtian.

Thickness: Thickness: It attains a thickness of 2m in the Dakhla Formation.

4.2. Total organic carbon (TOC)

The Total Organic Carbon (TOC) values vary significantly across the biozones, from CF9 to CF7 (1-32 sample), TOC values decreasing from 3% at sample 3 to remain relatively low, ranging between approximately 1% and 2%. Moving upward, in CF6 to CF4 (32-58 sample), TOC values begin to increase, reaching around 2% to 3%. Finally, in the upper zones, CF3 to CF1 (58-70 sample), TOC values peak at approximately 3% to 4% (Fig.4).

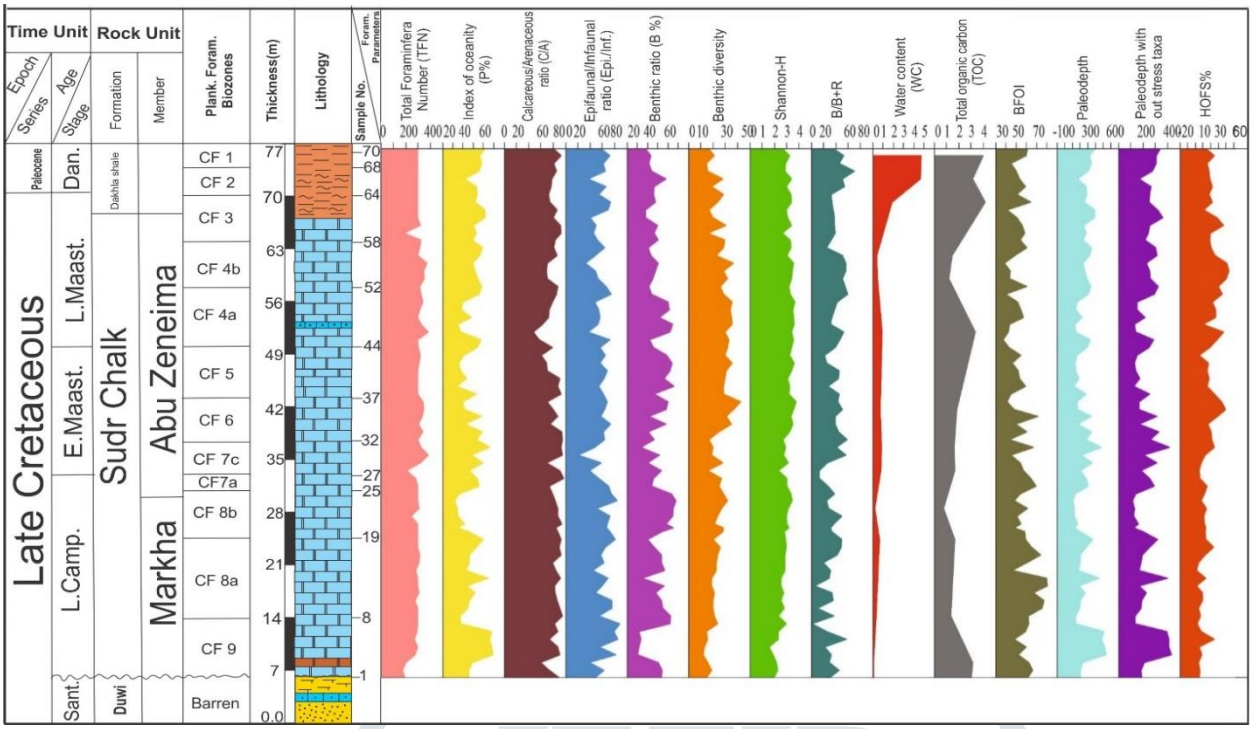


Fig.4. Calculated foraminiferal parameters, Water content, and Total organic carbon within the Nazzazat section.

4.3. Foraminiferal Parameters

Benthic foraminifera is regarded as an effective tool for estimating paleobathymetry (Table 1). Numerous studies have correlated depositional depths with faunal assemblages and individual species, largely based on foraminiferal parameters such as a) total foraminiferal number (TFN), which reflects water depth, with TFN generally increasing as water depth increases; and b) the benthic foraminiferal number (B), which serves as a valuable proxy for estimating past oxygen levels and organic matter flux (Fig. 4). Studies by Kaiho and Hasegawa (1994), Jorissen et al. (1995), Usami et al. (2013), Ortakand et al. (2015), and Sakai et al. (2021) have contributed to these methodologies.

4.3.1. Total Foraminifera Number (TFN)

The Total Foraminiferal Number (TFN) values show distinct variations across the biozones, reflecting changes in foraminiferal abundance and environmental conditions. TFN values range from 176 to 385 individuals in Campanian-Maastrichtian samples in the Gebel Nezzazat section. TFN values increase from 176 to 314 individuals within CF9 zone-CF8a subzone samples. In the CF8b subzone and CF7 zone, TFN values increase from 205 to 380 individuals. They subsequently rise once more in the CF6 and CF5 zones, reaching a maximum value of 350 individuals in CF6 zone samples and near the end of the CF5 zone (385 individuals) (Fig. 4).

4.3.2. Planktic Foraminifera Number (PFN)

The **(PFN)** values range from 190 to 80 individuals, from 65% to 30% (CF9 zone - CF8a subzone), where the values increase from 96 to 216 individuals in the CF8b subzone and CF7 zone, 40% to 70% then decrease again upward in CF6 and CF5 zones to reach a minimum value to 98 individuals in sample 59 in the end of CF3 zone (Fig. 4).

4.3.3. Benthic Foraminifera Number (BFN)

Values decrease rangang from 205 to 95 individuals (CF9 zone - CF8a subzone) in samples 1-19 (BFN). In the CF8b subzone and CF7 zone, (**BFN**) values increase from 110 to 213 individuals. They then rise once more in the CF6 and CF5 zones, reaching a peak of 240 individuals in sample 46 of zone CF4a (Fig. 4).

Table 1. Summary of paleo bathymetrical references of the most common benthic foraminiferal species used in the present study. **1-** Lüger,1985; **2-** Saint-Marc, 1992; **3-** Speijer,1994; **4-** Hewaidy et al., 2019; **5-** Speijer and Schmitz, 1998; **6-** Ernst et al. 2006; **7-** Sprong et al., 2012; **8-** El Dawy et al. 2018.

Most common benthic foraminiferal species	Bathymetric range				Ref.
	neritic			upper bathyal	
	inner	middle	outer		
Orthokarstenia spp.					4
Lenticulina spp.					4, 5, 7
Praebulimina spp.					1, 2
Bolivinoides spp.					2
Bolivina spp.					2
Nodosaria spp.					1, 5, 6, 7
Cibicidoides spp.					5, 7
Anomalinoides praeacutus					5, 7, 8
Gyroidinoides spp.					7
Gyroidinoides subangulata					7
Osngularia spp.					2, 5, 6, 7
Cibicidoides alleni					2, 3, 5
Gaudryina spp.					5, 8
Spiroplectinella spp.					3, 5
Anomalinoides affinis					5, 7
Neoflabellina spp.					1, 3
Lagena spp.					1
Tritaxia midwayensis					5
Pullenia cretacea					3, 5
Gyroidinoides globosus					5

4.3.4. Calcareous/Arenaceous Ratio (C/A)

In the Sudr Formation, calcareous foraminiferal tests make up the dominant component of the assemblage, accounting for 73–91%. This includes benthic calcareous genera such as *Lenticulina, Loxostomum, Gyroidinoides, Gavelinella, Bolivina, Cibicidoides, Bolivinoides, Orthokarestenia* and *Angulogavelinella*. In contrast, agglutinated forms are less common, comprising 9–22% of the assemblage, with taxa including *Gaudryina*, *Spiroplectinella*, *Clavulinoides*, *Ammodiscus*, *Pseudoclavulina*, *Tritaxia* and *Dorothia* (Fig. 4).

4.3.5. Epifaunal/Infaunal Ratio (E/I)

In the Nazzazat section, Epifaunal test ranges from 40% to 88%. In sample 5, this value is 55% and increase to reach 88% in sample 8 then decrease to 45% in sample 15 then increase to 80% in sample 24 and fluctuated to reach 85% at the end of the succession (Fig. 4).

4.3.6. Buliminids/Rotaliids (B/R)

The B/R ratios show a distanct variation at the base of the Sudr formation from CF9-CF8a, ranging from a minimum of 5% to a maximum of 60%.From CF8b start to increase until it drops again to reach about 10% and then stabilizes at relatively high levels (20-65%) for the rest of the the formation.

4.3.7. Diversity Indices and Shannon Index (H)

Diversity Indices of benthic foraminiferal species are widely used as indicators of paleoenvironment and paleobathymetry (e.g., Murray 2006; Murray and Alve, 2011). The Latest Campanian species richness varies from 15 to 29 in zones CF9 to CF8b respectively with **H Index** ranging from 1.5 to 2.9, the Maastrichtian ranges from 32 in zones CF7c and CF6 to 43, in zone CF5 about 36 and 37 in zone CF4 and **Shannon index values** ranging from 2.3 to 3.8 The Latest Maastrichtian ranges from 28 to 17 in zones CF2 and CF1 and **Shannon index values** ranges from 3.3 to 2.6 reflecting lower diversity (Fig. 4).

4.4. Paleodepth, Oxygen Concentrations and Species Distribution

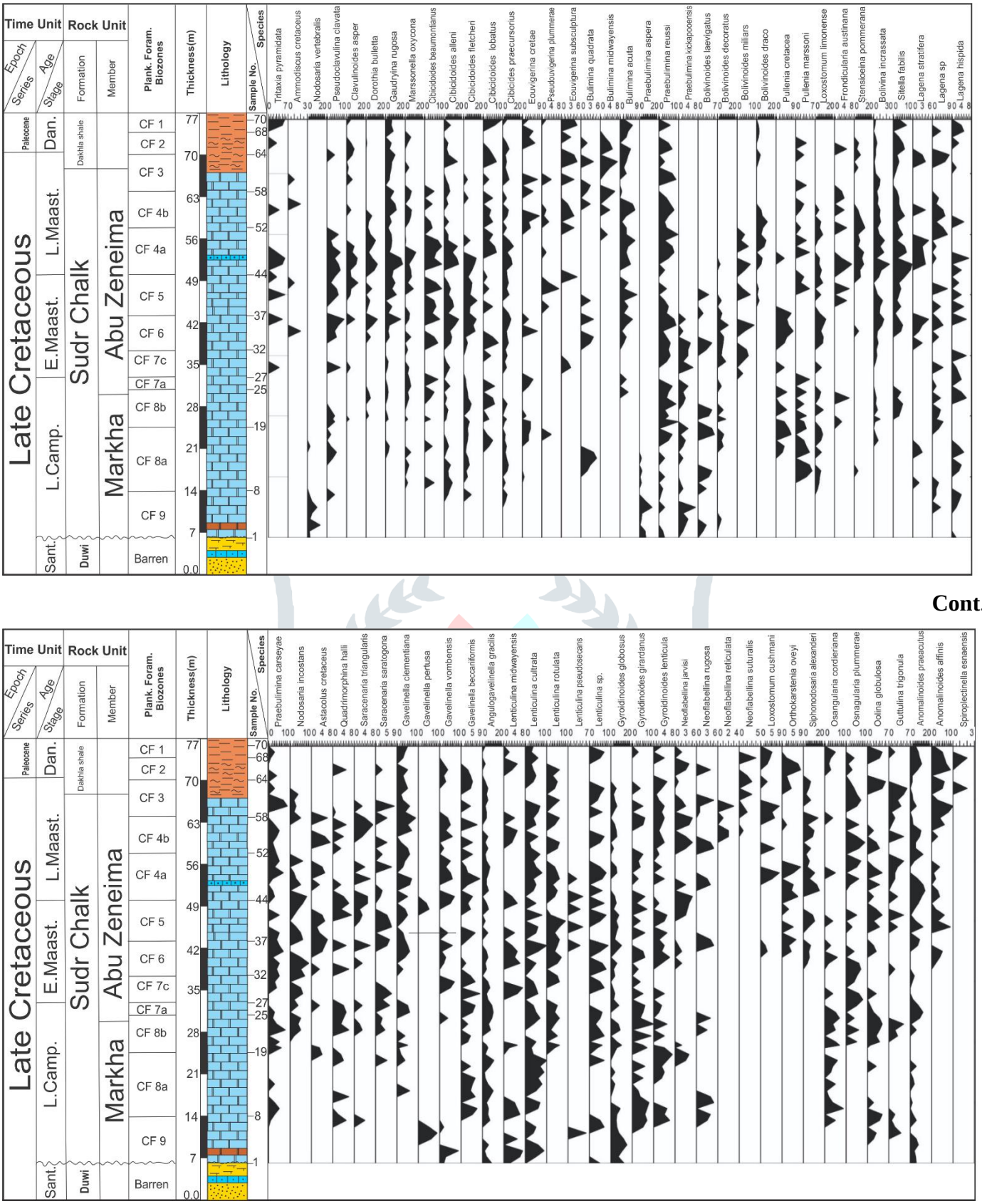
Based on the benthic assemblages, the highest inferred benthic foraminiferal paleodepth ranging from 201.6 to 539.84 m, was found in the late Campanian. While during the Campanian/Maastrichtian transition, the paleodepth increase varies from 143.74 to 455.24 m. Relatively high depth values ranging between 113.5 to 479.75 m have been estimated during Maastrichtian (Fig. 4).

The BFOI exhibited relatively higher values (ranging from 33.3 to 67.3, with an average of 50) during the Campanian, followed by a slight increase (from 35.71 to 79.5, with an average of 55) at the Campanian-Maastrichtian boundary. During the Maastrichtian, the values fluctuated between 40 and 60, with an average of 50 (Fig. 4). In contrast, the percentages of HOFS were relatively low throughout the Campanian (ranging from 4.5% to 9%) and began to gradually rise just below the Campanian-Maastrichtian boundary, reaching around 25%. During the Maastrichtian, the percentages fluctuated between 8% and 44%.

4.5. Benthonic foraminiferal biofacies

A total of 35 benthic foraminifera taxa were identified in the studied sections (Fig. 5a.b). Small species of *Praebulimina* are important taxa. The benthic foraminiferal assemblages of the Gebel Nazzazat section have relatively high productivity sequences that point to a major faunal shift around the Campanian/Maastrichtian boundary.

Buliminids comprise more than 40% of the benthic assemblage of the Campanian/Maastrichtian. *Praebulimina reussi* and *Praebulimina kickapooensis* are dominant species in the Campanian/Maastrichtian of the Gebel Nazzazat section. The dominance of *Praebulimina* is one of the most common genera in the (CF9-CF7c). Other species that are occasionally common are *Bolivina incrassata, Praebulimina reussi* and *Praebulimina kickapooensis, Gavelinella vombensis,* and *Angulogavelinella gracilis*. The *Praebulimina* inferred water depth of outer neritic to upper bathyal e.g., (Keller et al., 2002; Shirazi et al., 2014; Hewaidy et al., 2019).



Cont.

Fig.5. A distribution chart showing the relative abundances of common benthic foraminiferal taxa from the Nezzazzat Section.

Lenticulina is recorded in the lower part of the late Campanian (CF8a). It is explained by 6% of the total explained variance and dominated by abundant and common occurrences of *Lenticulina midwayensis, L. cultrata L. pseudosecans,* and *L. rotulata.* It reflects a middle to outer shelf between water depths from 50 to 100 m environments e.g., (Friedrich and Erbacher, 2006; Nouradini et al., 2015; Székely et al., 2017; Hewaidy et al., 2019).

Gyroidinoides is found in the chalky limestone at the upper part of CF9, the latest Campanian of the Sudr Formation, and the assemblages are characterized by *Gyroidinoides girardanus, G. subangulata, Praebulimina carseyae, P. reussi, P. kickapooensis, Cibicidoides beaumontianus, C. alleni, C. pseudoacutus* and *Angulogavelinella.* The *Gyroidinoides* assemblages are typically found in deeper water (bathyal) between paleo-water depths from 200 to 500 m e.g., (Miller et al., 2008; Sprong et al., 2013).

Bolivinoides are recorded mostly in the lower part of the Sudr Formation (CF8a), and the assemblages are dominated by *Bolivinoides laevigatus*; *B. miliaris,* and *B. decoratus*. While *Bolivinoides draco* starts to appear at CF5. The *Bolivinoides* reflect an outer neritic to bathyal environments e.g., (Alegret et al., 2003; Ashckenazi-Polivoda et al., 2017; Metwally et al., 2023).

Bolivina is recorded from the lower part of CF8b increasing obviously to the lower Maastrichtian Sudr Formation (CF6) and the assemblages are characterized by dominated *Bolivina incrassate, Bolivinoides decoratus, Frondicularia austinana* and *Angulogavelinella gracilis,* which refers to an outer neritic environment (Jaff et al., 2014; Farouk and Jain, 2016; Jain and Farouk, 2017; Bejaoui et al., 2019; Taha and Ali, 2024).

Orthokarestenia is recorded from the early Maastrichtian Sudr Formation (CF6). It is characterized by the common occurrences of assemblages *Orthokarestenia oveyi. Cibicidoides alleni,* and *C. beaumontianus*. It reflects an inner to middle neritic environments shelf between water depths abundant from 40 to 100 m environments (Székely et al., 2017; Bălc et al., 2024). The CF6 Zone of the Sudr Formation contains abundant buliminids such as *Bulimina acuta, B. qudatra* and *Praebulimina reussi.*

Nodosaria is recorded from the upper Campanian Sudr Formation (CF9) and is characterized by *Nodosaria vertebrails,* which are only founded at CF9, while *N. obscura, Frondicularia austinana, Lenticulina discrepans, L. midwayensis, L. rotulata, Ramulina pseudoaculeata, Lagena striatifera,* and *Astacolus cretaceous* from CF8. It reflects shallow-middle neritic paleoenvironments (Szinger, 2008; Hewaidy et al., 2019).

Cibicidoides is found increasing in the chalky limestone at the upper Maastrichtian part of the Sudr Formation from (CF5 to CF4a), and the assemblage is characterized by *Cibicidoides alleni, C. fletcheri, Bolivina incrassata, Bolivinoides draco, B. miliaris, Pseudoclavulina clavate, Stensioeina pommerana,*

Praebulimina carseyae, and P. reussi. The *Cibicidoides* are typically found in outer neritic to upper bathyal environments (Miller et al., 2008; Katz et al., 2018; Metwally et al., 2023).

Spiroplectinella biofacies are found at the Late Maastrichtian part of the formation (CF3 to CF1). It is associated with *Spiroplectinella esnaensis*, *Gaudryina rugosa* and *Clavulinoides asper*. It can be founded from outer neritic to upper bathyal environment.(El-Dawy 2001; Farouk and Jain 2016).

The calcareous foraminifera of the upper part of the Sudr Formation CF3 Zone is represented by a high content of *Gyroidinoides girardanus, G. lenticula Cibicidoides praecursorius, Osangularia cordieriana, Anomalinoides praeacutus, Orthokarstenia oveyi*, while the agglutinated formainifera *are Spiroplectinella esnaensis* and *Gaudryina rugosa*. Other species that are commonly found in the Sudr Formation include *Anglogavelinella gracilis, Gavelinella clementiana and G. vombensis*. The common buliminids in this interval are *Bolivinoide draco, Eouvigerina cretae* and *E. subsculptura* (Fig. 5a,b).

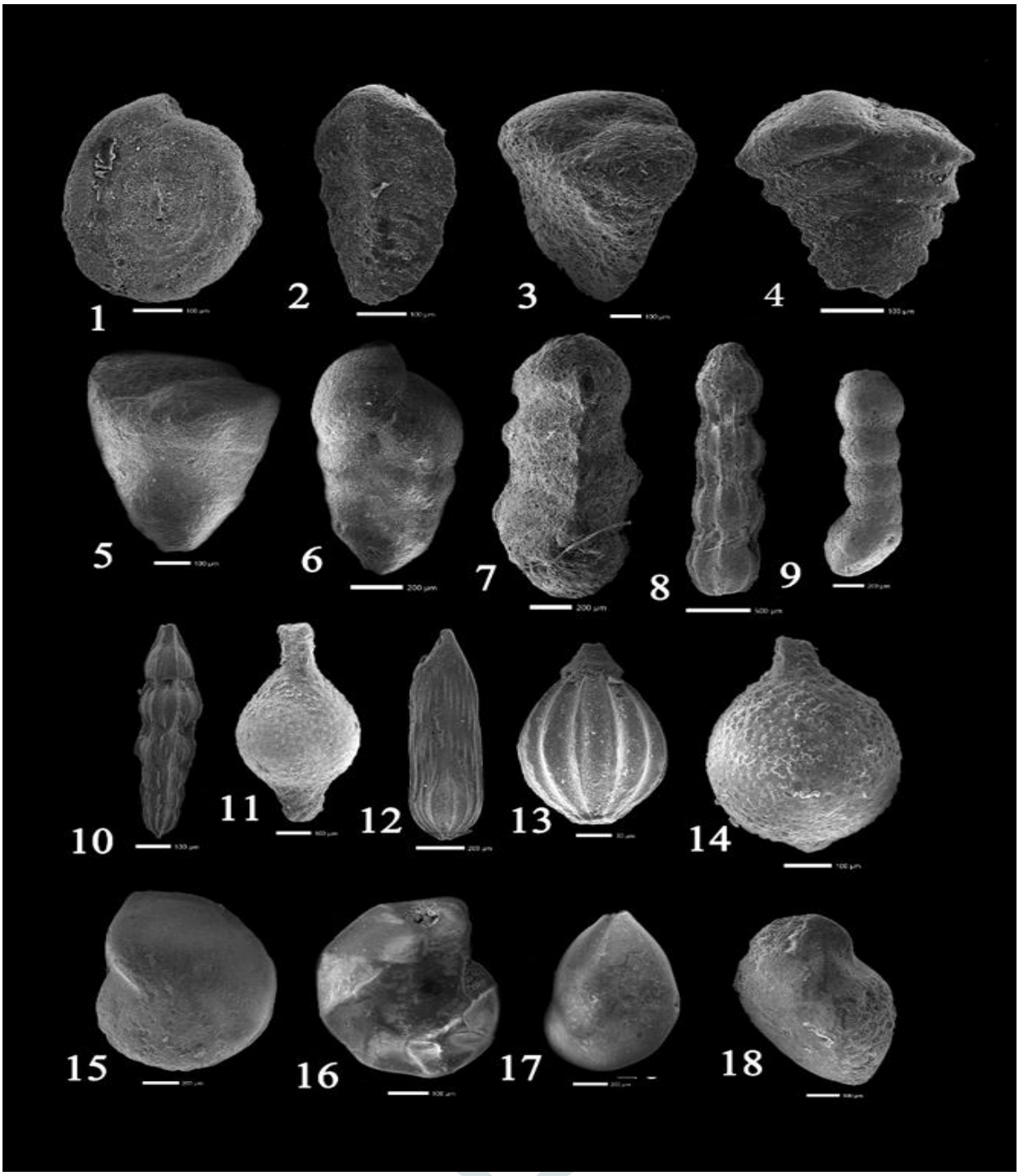


Plate 1. SEMs of important benthic foraminiferal species.(1) *Ammodiscus cretaceus* (Reuss), sample 60, CF3 Zone; **(2)** *Spiroplectinella dentate* (Alth), sample 28, CF7c Zone; **(3)** *Gaudryina rugosa* (d'Orbigny), sample 24, CF8b Zone; **(4)** *Spiroplectinella esnaensis* (LeRoy), sample 63, CF3 Zone; **(5)** *Marssonella oxycona* (Reuss), sample 67, CF2 Zone; **(6)** *Dorothia bulletta* (Carsey), sample 46, CF4b Zone; **(7)** *Tritaxia pyramidata* Reuss, sample 69, CF1 Zone; **(8)** *Nodosaria vertebralis* (Batsch, 1781), sample 16 CF8a; **(9)** *Pseudoclavulina clavata* (Cushman), sample 22, CF8b Zone; **(10)** *Nodosaria obscura (*Reuss), sample 39, CF5 Zone; **(11)** *Ramulina pseudoaculeata* (Olsson), sample 64, CF3 Zone; **(12)** *Frondicularia austinana* Cushman, sample 45, CF4a Zone; **(13)** *Lagena striatifera* Tappan, sample 57, CF4b Zone; **(14)** *Lagena striatifera* Tappan, sample 57, CF4b Zone; **(15)** *Lenticulina navicula* (d'Orbigny, 1840), sample 18, CF8a Zone; **(16)** *Lenticulina midwayensis (Plummer, 1927),*sample 20, CF8b Zone; **(17)** *Saracenaria triangularis* (d'Orbigny), sample 23, CF8b Zone; **(18)** *Saracenaria saratogona* (d'Orbigny), sample 18, CF8a Zone.

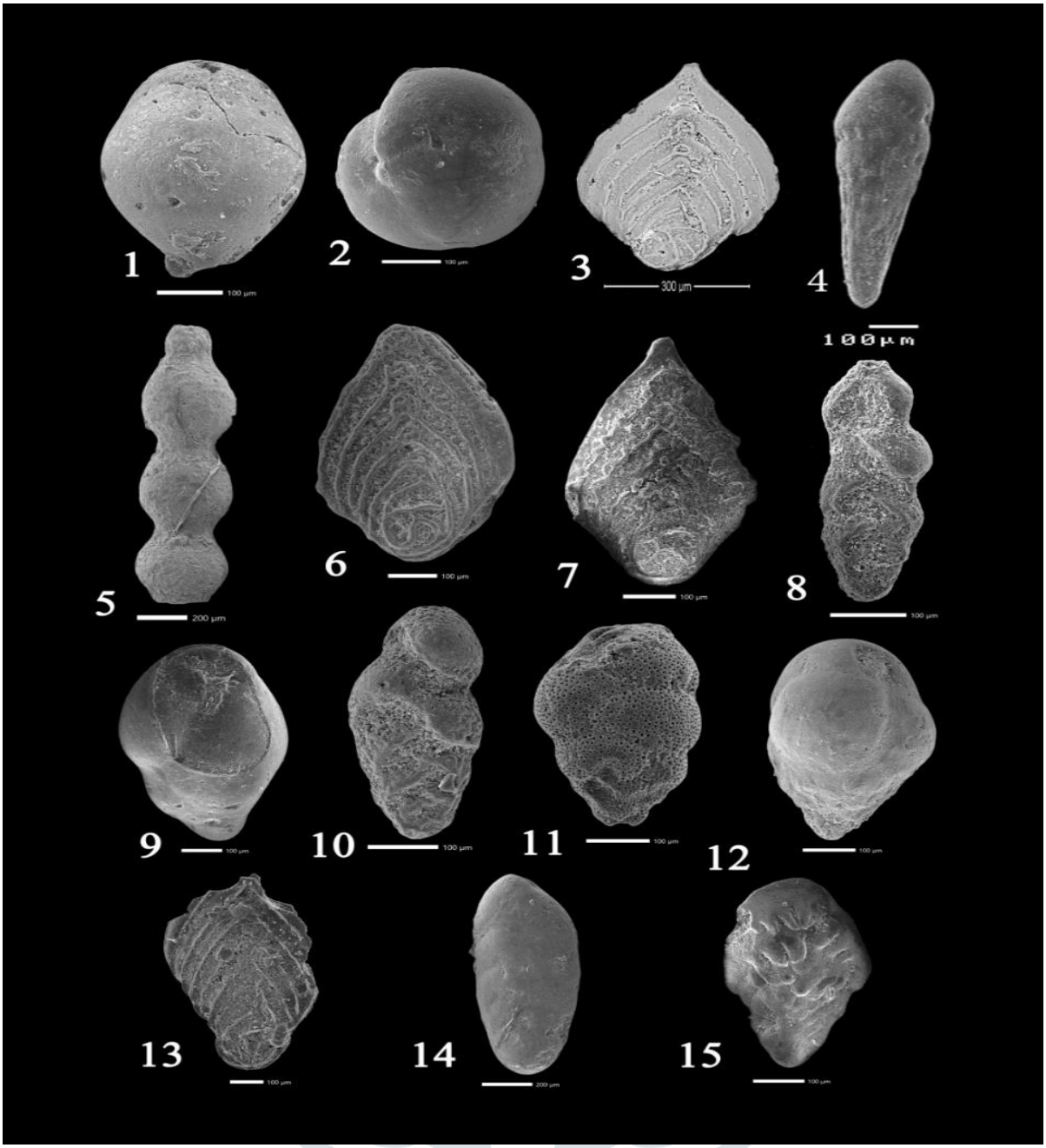


Plate 2. (1) *Oolina globulosa* (Montagu), sample 2, CF9 Zone; **(2)** *Pullenia marssoni (Cushman & Todd, 1943)* sample 66, CF2 Zone; **(3)** *Neoflabellina suturalis* (Cushman, 1935), sample 65, CF4b Zone; **(4)** *Loxostomum cushmani* Wickenden, sample 69, CF1 Zone; **(5)** *Siphonodosaria alexanderi* (Cushman), sample 64, CF3 Zone; **(6)** *Neoflabellina rugosa* (d'Orbigny), sample 48, CF4a Zone; **(7)** *Neoflabellina jarvisi* (Cushman), sample 57, CF4b Zone; **(8)** *Eouvigerina subsculptura* MacNeil and Caldwell, sample 67, CF2 Zone; **(9)** *Praebulimina reussi* (Morrow), sample 32, CF7c Zone; **(10)** *Eouvigerina cretae (Ehrenberg, 1854)*, sample 68, CF2 Zone;(11) *Bulimina incisa (Cushman, 1926)*, sample 40, CF5 Zone; **(12)** *Praebulimina carseyae* (Plummer), sample 54, CF4b Zone; **(13)** *Neoflabellina rugosa* (d'Orbigny), sample 66, CF2 Zone; **(14)** *Bolivina incrassata gigantea* Wicher, sample 22, CF8b Zone; **(15)** *Bolivinoides decoratus* (Jones), sample 16, CF8a Zone.

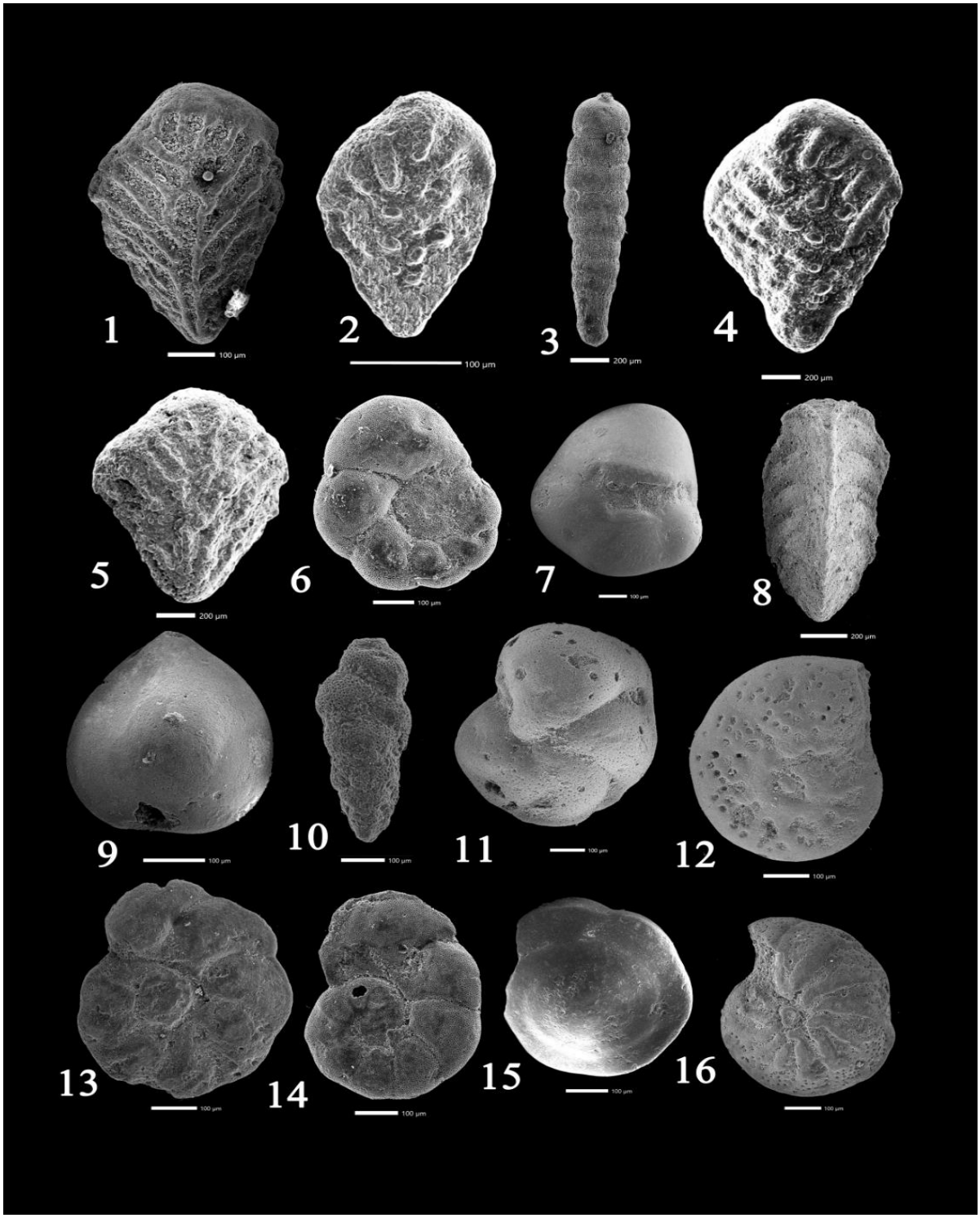


Plate 3. (1) *Bolivinoides draco* (Marsson), sample 46, CF4a Zone; (2) *Bolivinoides laevigatus(* Marie), sample 32, CF7c Zone; (3) *Orthokarstenia oveyi (Nakkady, 1950)*sample 38, CF5 Zone; (4) *Bolivinoides decoratus* (Jones), sample 46, CF4a Zone; (5) *Bolivinoides miliaris* (Hiltermann and Koch), sample 32, CF7c Zone; (6) *Valvulineria quadrimorphin* Cushman, sample 62, CF3 Zone; (7) *Quadrimorphina halli* (Jennings), sample 23, CF8b Zone; (8) *Clavulinoides asper* (Cushman), sample 44, CF5 Zone; (9) *Guttulina trigonula* (Reuss), sample 24, CF8b Zone; (10) *Pseudouvigerina cretacea* Cushman, sample 68, CF2 Zone; (11) *Cibicides beaumontianus* (d'Orbigny), sample 24, CF8b Zone; (12) *Cibicides fletcheri* Galloway and Wissler, sample 17, CF8a Zone; (13) *Cibicides lobatulus* (Walker and Jacob), sample 69, CF1 Zone; (14) *Cibicides subcarinatus (*Cushman and Deaderick, D.V), sample 68, CF2 Zone; (15) *Osangularia plummerae* Brotzen, sample 68, CF2 Zone; (16) *Angulogavelinella gracilis* (Marsson, 1878) sample 47, CF4a Zone

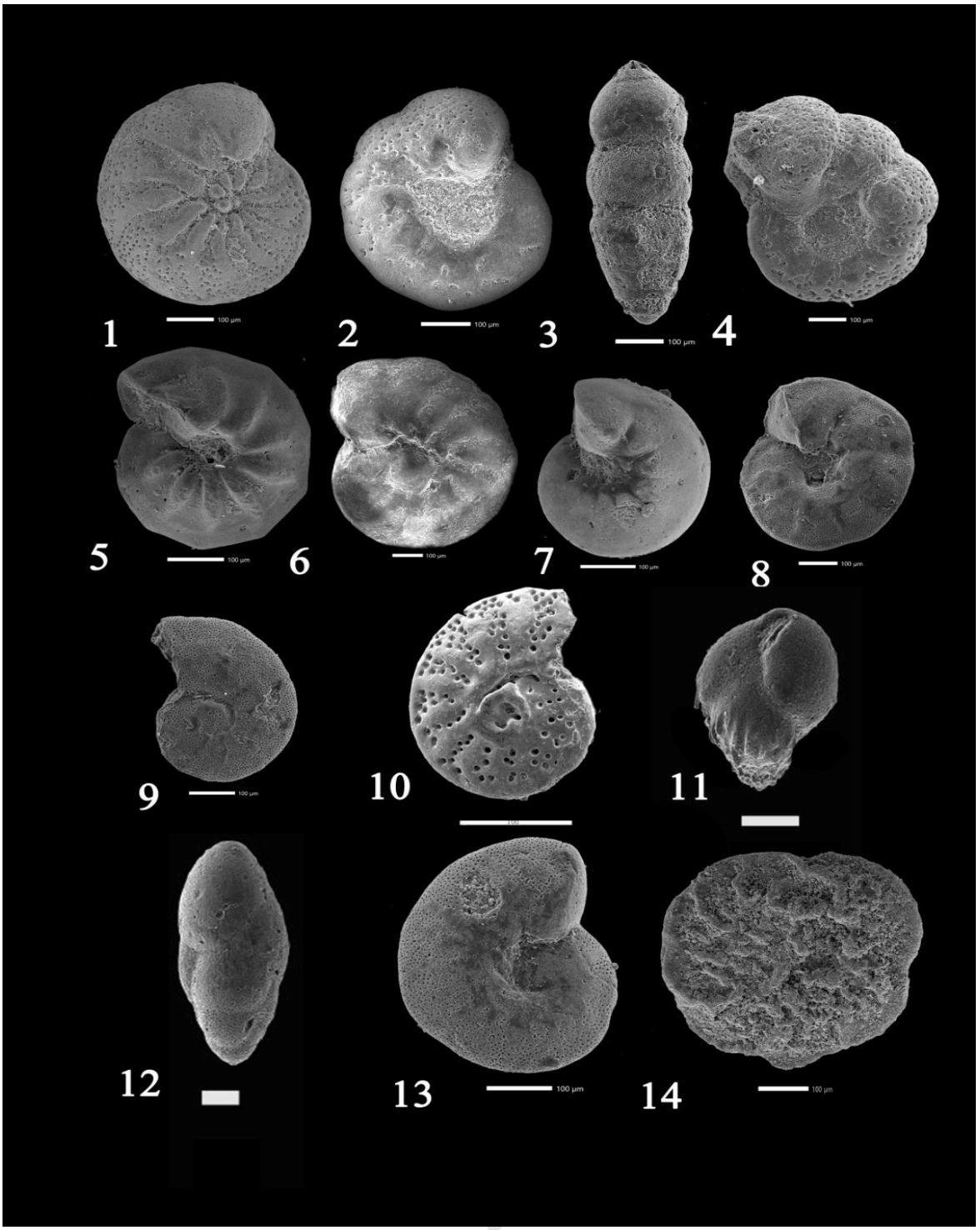


Plate 4. (1) *Angulogavelinella gracilis* (Marsson, 1878), sample 11, CF8a Zone; (2) Gavelinella clementiana (d'Orbigny)sample 38, CF5 Zone; (3) *Pseudonodosaria manifesta* (Reuss), sample 64, CF3 Zone;(4) *Gavelinella vombensis* (Brotzen), sample 36, CF5 Zone; (5) *Gyroidinoides girardanus* (Reuss, 1851), sample 63, CF3 Zone; (6) *Stensioneina pommerana* Brotzen, sample 12, CF8a Zone; (7) *Gyroidinoides globosus (Hagenow, 1842)*, sample 61, CF3 Zone; (*8) Gyroidinoides lenticula* (Reuss) V.V, sample 68, CF2 Zone; (9) *Anomalinoides praeacutus* D.V, sample 26, CF7c Zone; (10) Gavelinella acuta (Plummer), sample 33, CF6 Zone (11) *Bulimina midwayensis* (Cushman and Parker), sample 65, CF2 Zone; (12) *Bulimina quadrata* (Plummer), sample 48, CF4a Zone; (13) *Gavelinella brotzeni (*Said and Kenway V.V), sample 59, CF3 Zone; (14) *Stensioneina pommerana* Brotzen, sample 45, CF4a zone.

5. DISCUSSION

Benthic Foraminifera and Upwelling System

Through the present study, benthic foraminferal assemblages and paramerters during the Campanian succession (CF9 to CF8a zones) is interpreted to have been deposited in outer neritic to upper bathyal environments, with water depths decreasing from approximately 500 to 200 meters. These conditions were characterized by relatively well-oxygenated bottom waters with low organic carbon flux to the seafloor, reflecting a more oligotrophic environment. The environment is also distinguished by relatively low values of TFN, BFN, species diversity, and the Shannon index, which overall increase upward.

During the Campanian, high Benthic Foraminiferal Oxygen Index (BFOI) and relatively low Total Organic Carbon (TOC) values indicate limited preservation of organic matter, and a high abundance of epifaunal species. (Olsson and Nyong 1984; Speijer and Schmitz 1998; Farouk et al.,2024).
Additionally, the low estimates for Buliminds / Buliminds + Rotaloidids (Ashckenazi 2017) further support the interpretation of well-oxygenated conditions. Buliminds are generally more abundant in environments with moderate to low oxygen levels, so their reduced presence suggests a lack of significant oxygen stress at the seafloor. Similarly, the low relative abundance of Buliminds + Rotaloidids reflects the oligotrophic conditions of the Campanian, where nutrient availability and organic flux to the seafloor were relatively low. The benthic foraminiferal assemblage was dominated by species adapted to these well-oxygenated and low organic carbon environments.(Ashckenazi et al.,2017)

The transition from the Campanian to Maastrichtian (CF8b to CF7) is marked by a deepening of the water column from 140 to 455 m and a shift towards outer neritic to deeper bathyal settings, which corresponds with a decrease in the preservation of organic carbon and relatively low TOC values (2-3%), also this transition showed high BFOI and relatively low HOFS accompanied by highly calcified epifaunal taxa.(Li et al.,1999; Sherif et al.,2024).

The Maastrichtian succession (CF6 to CF4a), based on benthic foraminiferal assemblages and the parameters, suggests a shallower depositional setting from 130 to 340 m maximum that is outer neritic. This interval is also marked by a general rise in benthic diversity, TFN, and HFOS, along with a decline in BFOI.

These changes indicate a decrease in oxygen availability at the seafloor, linked to an increase in organic matter, as evidenced by a slight reduction in sediment-dwelling epifaunal taxa and increasing B/B+R ratio.This interval is associated with the onset of upwelling conditions, as indicated by an increase in benthic foraminiferal numbers (BFN), increasing diversity and the dominance of deep-water species such as Praebulimina and Bolivina, which are indicative of low-oxygen environments typical of upwelling zones.

During the upper Maastrichtian (from CF4b to CF1), the depositional environment deepens to around 400 meters (upper bathyal), reflecting an increase in ocean depth. This period is characterized by rising levels

of HOFS (High Organic Flux Sediments), Total Organic Carbon (TOC), and B/B+R, while the Benthic Foraminiferal Oxygen Index (BFOI) decreases, indicating upwelling conditions.

The increase in calcareous foraminifera, such as *Cibicidoides* and *Gyroidinoides*, suggests a stable depositional environment with enhanced organic matter accumulation, driven by ongoing upwelling. This upwelling would have facilitated the influx of nutrients, which in turn supported higher primary productivity and organic carbon deposition in the deeper waters.

Further changes in the calcareous/arenaceous ratio (C/A) and the dominance of foraminiferal species like *Praebulimina*, *Gyroidinoides*, and *Bolivinoides* provide additional evidence of significant paleoenvironmental shifts during this time. These shifts align with a dynamic marine system influenced by periodic upwelling, which promoted increased nutrient availability, boosting productivity and enhancing organic carbon accumulation in the sedimentary record.

During the Late Cretaceous, the southern Tethyan Ocean along Egypt's continental shelf experienced nutrient-rich conditions due to intense coastal upwelling (Eladawy et al., 2017; Fathy et al., 2023). Organic-rich sediments from both the early and late Maastrichtian were deposited under different environmental conditions. The early Maastrichtian sediments formed primarily under an anoxic water column, while the late Maastrichtian sediments were deposited under an anoxic/dysoxic marine environment.(Fathy et al.,2023).

The identified benthic foraminifera taxa provide further insights into past environmental conditions and bathymetry. Species such as *Praebulimina reussi* and *Praebulimina kickapooensis* are dominant in the Campanian-Maastrichtian boundary interval, suggesting outer neritic to upper bathyal environments. These species are typically associated with middle to outer shelf settings, indicating that the study area was influenced by outer shelf to bathyal water depths during this period. The presence of other species such as *Bolivinoides*, *Cibicidoides*, and *Gyroidinoides* further corroborates the interpretation of outer neritic to bathyal depths, with specific species showing affinities for deeper, more oxygenated waters. The dominance of *Gyroidinoides* and *Cibicidoides* at the upper Maastrichtian (CF5–CF4a) suggests that the study area was in an upper bathyal environment during this interval, with species that thrive in more open ocean conditions.

6. CONCLUSION

The study of benthic foraminiferal assemblages within the Campanian-Maastrichtian intervals of the Sudr Formation in West-Central Sinai, Egypt, provides crucial insights into paleoenvironmental conditions, water depth, and oxygenation levels during this time. Nine planktonic foraminiferal zones are recorded through the Nezzazat section, ranging from CF9 to CF1. Nine benthic biofacies are distinguished, reflecting fluctuations in paleowater depth, from outer neritic to upper bathyal settings (Bulimina, Lenticulina, Gyroidinoides, Bolivinoides, Bolivina, Orthokarstenia, Nodosaria, Cibicidoides, and Spiroplectinella). The observed changes in foraminiferal assemblages, such as variations in the Total Foraminiferal Number (TFN)

and Benthic Foraminiferal Number (BFN), highlight dynamic shifts in depositional settings and oceanographic conditions. These shifts reflect a transition from less productive, well-oxygenated environments in the Campanian to more productive, upwelling-influenced conditions in the Maastrichtian. The dominance of foraminiferal taxa such as Praebulimina and Bolivina, along with decrease in diversity and the Benthic Foraminiferal Oxygen Index (BFOI), further suggest a marked intensification of upwelling during this time, supporting a higher organic carbon flux to the seafloor. The transition in species composition and the increase in deep-water taxa during the Maastrichtian point to changes in nutrient availability, possibly linked to shifts in sea level or ocean circulation patterns. Finally, these findings underscore the critical role of upwelling in shaping marine ecosystems and influencing organic carbon deposition during the late Cretaceous, offering a clearer understanding of the complex interplay between environmental factors and biological productivity during this period.

REFERENCES

Abbass, H.L., 1962. A monograph on the Egyptian Cretaceous pelecypods. Geological Survey Mineral Research Dept. 1:1–224.

Abdalla Shahin. Integrated foraminiferal biostratigraphy, bioevents and sea-level reconstruction in the Campanian–Maastrichtian succession at Gabal Nezzazat, south-western Sinai, Egypt. Geological Journal. 2022;1–25. DOI: 10.1002/gj.4634

Aguiar, E. J., Morgan, P. J., Collins, C. E., Plotnikoff, R. C., Callister, R., 2014. Efficacy of interventions that include diet, aerobic and resistance training components for type 2 diabetes prevention: a systematic review with meta-analysis. International Journal of Behavioral Nutrition and Physical Activity, 11, 1-10.

Alegret, L., Molina, E., Thomas, E., 2003. Benthic foraminiferal turnover across the Cretaceous/Paleogene boundary at Agost (southeastern Spain): paleoenvironmental inferences, Marine Micropaleontology. 48 (3-4), 251- 279.

Arz, J.A., Molina, E., 2002. Bioestratigrafiay cronoestratigrafiacon foraminiferos planctonicos del Campaniense superiory Maastrichtiense de latitudes subtropicalesy templadas (Espana, Francia, y Tunicia). Neues Jb Geol. Palaontol. Abh. 224:161-195.

Ashckenazi-Polivoda, S., Edelman-Furstenberg, Y., Almogi-Labin, A., Benjamini, C., 2010. Characterization of lowest oxygen environments within ancient upwelling environments: Benthic foraminifera assemblages. Palaeogeography, Palaeoclimatology, Palaeoecology, 289(1-4), 134-144.

Ashckenazi-Polivoda, S., Titelboim, D., Meilijson, A., Almogi-Labin, A., Abramovich, S., 2017. Bathymetric trend of Late Cretaceous southern Tethys upwelling regime based on benthic foraminifera. Cretaceous Research, 82, 40-55.

Avila-Alonso, D., Baetens, J. M., Cardenas, R., De Baets, B. (2020). Oceanic response to the consecutive Hurricanes Dorian and Humberto (2019) in the Sargasso Sea. Natural Hazards and Earth System Sciences Discussions, 2020, 1-29.

Avnaim-Katav, S., Hyams-Kaphzan, O., Milker, Y. and Almogi-Labin, A., 2015. Bathymetric zonation of modern shelf benthic foraminifera in the Levantine Basin, eastern Mediterranean Sea. Journal of Sea Research, 99: 97-106.

Bălc, R., Bindiu-Haitonic, R., Kövecsi, S. A., Vremir, M., Ducea, M., Csiki-Sava, Z., ... Vasile, Ș., 2024. Integrated biostratigraphy of Upper Cretaceous deposits from an exceptional continental vertebrate-bearing marine section (Transylvanian Basin, Romania) provides new constraints on the advent of 'dwarf dinosaur'faunas in Eastern Europe. Marine Micropaleontology, 187, 102328.

Bartov, Y., Steinitz, G., 1977. The Judea and Mount Scopus groups in the Negev and Sinai with trend surface analysis of the thickness data. Isr. J. Earth Sci., vol. 61, p. 119-148.

Bejaoui, A., Saidi, E., Zaghbib-Turki, D., 2019. Small benthic foraminiferal biostratigraphy and palaeoecology during the Campanian-Maastrichtian transition in north-western Tunisia. Turkish Journal of Earth Sciences, 28(4), 500-530.

Bernhard, J.M., 1986. Characteristic assemblages and morphologies of benthic foraminifera from anoxic, organic-rich deposits; Jurassic through 88 Holocene. Journal Foraminifera Research, 16:207–215. https://doi.org/10.2113/gsjfr.16.3.207

Camoin, G., Bellion, Y., Benkhelil, J., Cornee, J.J., Dercourt, J., Guiraud, R., Poisson, A., Vrielynck, B., 1993. Late Maastrichtian palaeoenvironments (69.5–65 My). In: Dercourt, J., Ricou, L.E., Vrielynck, B. (Eds.), Atlas Tethys Paleoenvironmental Maps. BEICIP-FRANLAB, Rueil-Malmaison.

Cao, Z., Dai, M., Evans, W., Gan, J., Feely, R., 2014. Diagnosing CO 2 fluxes in the upwelling system off the Oregon–California coast. Biogeosciences, 11(22), 6341-6354.

Caron, M., 1985. Cretaceous planktic foraminifera, in Plankton Stratigraphy edited by Bolli, H. M.; Sautiders, J. B. and Perch-Nielsen, K. Cambridge Univ. Press., p. 17-86, Cambridge.

Cherif, O. H.; Al Rifaiya, I. A.; Ai Afifi, F. I. and Orabi, H. O., 1989. Planktonic foraminifera and chronostratigraphy of Senonian exposures in West-Central Sinai, Egypt. Rev. Micropaleontology, 32 (2), 167-184.

Corliss, B. H., C. Chen., 1988. Morphotype Patterns of Norwegian Sea Deep-Sea Benthic Foraminifera and Ecological Implications. *Geology* 16 (8): 716–19.https://doi.org/10.1130/00917613(1988)016<0716:MPONSD>2.3.CO;2.

Corliss, B.H., 1985. Microhabitats of benthic foraminifera within deep-sea sediments. Nature 314:435. https://doi.org/10.1038/ 314435a0

Corliss, B.H., 1991. Morphology and microhabitat preferences of benthic foraminifera from the Northwest Atlantic Ocean. Mar. Micropaleontol. 17, 195–236.

De Rijk, S., Troelstra, S. R., & Rohling, E. J. (1999). Benthic foraminiferaldistribution in the Mediterranean Sea. Journal of Foraminiferal Research, 29, 93–103.

Dercourt, J., Ricou, L.E., Vrielynck, B. (Eds.), 1993. Atlas Tethys Paleoenvironmental Maps. Beicip-Franlab, Rueil-Malmaison.

Donnadieu Y, Puceat E, Moiroud M, Guillocheau F, Deconinck J-F (2016) A better-ventilated ocean triggered by Late Cretaceous changes in continental configuration. Nat Commun 7:10316. https:// doi. org/ 10. 1038/ ncomm s10316

Douglas RG (1973). Benthonic foraminiferal biostratigraphy in the central north Pacific, Leg 17, deep sea drilling project. Initial Rep Deep Sea 17: 607-671.

El Shazly, E. M., 1977. The geology of the Egyptian region In: A. E. N. Nairn, W. H. Kanes and F. G. Stehli (Eds.). The Ocean Basins and Margins, vol. 4b, the Eastern Mediterranean. Plenum Press, New York, NJ, 379-444.

Eladawy, A.; Nadaoka, K.; Negm, A.; Abdel-Fattah, S.; Hanafy, M.; Shaltout, M. Characterization of the northern Red Sea's oceanic features with remote sensing data and outputs from a global circulation model. *Oceanologia* 2017, *59*, 213−237.

El-Ayaat, A., Khalifa, M. A., 2010. Lithostratigraphy, facies analysis, paleoenvironments and cyclicity of the upper Cretaceous (Cenomanian-Santonian) mixed carbonate-siliciclastic sequence in north Eastern Desert. In Egypt. 5th Inter Conf Geol Tethys Realm South Valley Univ (Vol. 421, p. 444).

Ernst, S., van der Zwaan, B., 2004. Effects of experimentally induced raised levels of organic flux and oxygen depletion on a continental slope benthic foraminiferal community. Deep Sea Research Part I: Oceanographic Research Papers, 51(11), 1709-1739.

Farouk, S., Bazeen, Y., Ahmed, f., Elarmi, Z., Al kahtany, K., Frontalini, F.,Zaky, A., 2024. The Campanian-Maastrichtian benthic foraminiferal assemblages at the Elles section (Tunisia): A perspective for paleoenvironmental, paleobathymetric and sea-level fluctuation reconstruction ناقص اسم المجله

Farouk, S., Faris, M., Bazeen, Y. S., Elamri, Z., Ahmad, F., 2021. Upper Campanian-lower Maastrichtian integrated carbon isotope stratigraphy and calcareous microplankton biostratigraphy of North-central Tunisia. Marine Micropaleontology, 166, 102003.

Farouk, S., Jain, S., 2016. Benthic Foraminiferal Response to Relative Sea-level Changes in the Maastrichtian-Danian Succession at the Dakhla Oasis, Geological Magazine, Western Desert, Egypt, 1-18.

Farouk, S., Jain, S., Al-Kahtany, K., Ahmad, F., Abdeldaim, A., 2023. Relationship of Maastrichtian-Thanetian benthic foraminiferal species diversity, palaeooxygenation, and palaeoproductivity in shallow waters of the Western Desert, Egypt. Geo-Marine Letters, 43(1), 4.

Farouk,S. Maastrichtian carbon cycle changes and planktonic foraminiferal bioevents at Gebel Matulla, west-central Sinai, Egypt, Cretac. Res. 50 (2014) 238–251.

Fatela, F., Taborda, R., 2002. Confidence limits of species proportions in microfossil assemblages. Marine Micropaleontology. 45:169–174. https:// doi. org/ 10.1016/S0377-8398(02)00021-X

Fathy, D.; Abart, R.; Wagreich, M.; Gier, S.; Ahmed, M. S.; Sami, M. Late Campanian Climatic-Continental Weathering Assessment and Its Influence on Source Rocks Deposition in Southern Tethys, Egypt. *Minerals* 2023, *13*, 160.

Fathy, D.; Wagreich, M.; Gier, S.; Mohamed, R. S. A.; Zaki, R.; El Nady, M. M. Maastrichtian oil shale deposition on the southern Tethys margin, Egypt: Insights into greenhouse climate and paleoceanography. *Palaeogeogr., Palaeoclimatol., Palaeoecol.* 2018, *505*, 18−32.

Friedrich, O., Erbacher, J., 2006. Benthic foraminiferal assemblages from Demerara Rise (ODP Leg 207, western tropical Atlantic): possible evidence for a progressive opening of the Equatorial Atlantic Gateway, Cretaceous Research. 27 (3), 377–397.

Friedrich, O., Hemleben, C., 2007. Early Maastrichtian benthic foraminiferal assemblages from the western North Atlantic (Blake Nose) and their relation to paleoenvironmental changes. Marine Micropaleontology 62: 31-44.

Friedrich, O., Reichelt, K., Herrle, J.O., Lehmann, J., Pross, J., Hemleben, C., 2003. Formation of the Late Aptian Niveau Fallot black shales in the Vocontian Basin (SE France): evidence from foraminifera, palynomorphs, and stable isotopes. Marine Micropaleontology 49, 65-85.

Friedrich, O., Schmiedl, G., Erlenkeuser, H., 2006. Stable isotope composition of Late Cretaceous benthic foraminifera from the southern South Atlantic: Biological and environmental effects. Marine Micropaleontology, 58: 135-157.

Frontalini, F., Rostami, M.A. and Coccioni, R., 2016. Paleobathymetric assessments of the upper Albian-lower Danian Gubbio section (Italy). Geological Society of America Special Papers, 524: SPE524-08.

Ghorab, M. A., 1961. Abnormal stratigraphic features in Ras Gharib oil field. 3 rd Arab. Petr. Congr., 110 p. Alexandria.

Gibson, T. G., 1989. Planktic: benthic foraminiferal ratios: Modern patterns and Tertiary applicability: Marine Micropaleontology, 15, 29–52.

Haq, B.U., 2014. Cretaceous eustasy revisited. Glob. Planet. Chang. 113, 44–58. https:// doi.org/10.1016/j.gloplacha.2013.12.007

Hewaidy, A. G. A., Farouk, S., Mandur, M. M., El Agroudy, I. S., 2019. Planktonic foraminiferal and paleoenvironments of the upper Campanian-Maastrichtian succession in Wadi Qena, Egypt. Egyptian Journal of Petroleum, 28(1), 47-59.

Hewaidy, A., Farouk, S., EL-Balkiemy, A.F., Foraminiferal biostratigraphy, stage boundaries and paleoecology of the uppermost Maastrichtian-Lower Eocene succession at Esh E-Mellaha area, north eastern Desert, Egypt, J. Am. Sci. 13 (5) (2017) 73–113.

Huber BT, MacLeod KG, Watkins DK, Coffin MF (2018) The rise and fall of the Cretaceous Hot Greenhouse climate. Glob Planet Change 167:1–23

Huber, B.T., Norris, R.D., MacLeod, K.G., 2002. Deep-sea paleotemperature record of extreme warmth during the Cretaceous. Geology 30, 123–126. https://doi.org/ 10.1130/0091-7613(2002)030<0123:DSPROE>2.0.CO;2.

Ioannou, A., Speich, S., Laxenaire, R., 2022. Characterizing mesoscale eddies of eastern upwelling origins in the Atlantic Ocean and their role in offshore transport. Frontiers in Marine Science, 9, 835260.

Ismail, A. A., El-Saadany, M. A., 1995. Some Cretaceous foraminifera from northern Sinai, Egypt. Middle East Research Center, Ain Shams University, Earth Science Series, 9, 173-203.

Issawi, B., Francis, M., Youssef, A.A., Osman, A., 2009. The Phanerozoic Geology of Egypt: A geodynamic approach. Ministry of Petroleum, The Egyptian Mineral Resources Authority. Special Publication No.81, 589 pp.

Issawi, B., Sallam, E. S., Salem, M., 2018. Tectonostratigraphic and sedimentary evolution of the Ubur–Orabi sub-basin, southeast Nile Delta, Egypt. Carbonates and Evaporites, 33, 663-681.

Jaff, R. B., Williams, M., Wilkinson, I. P., Lawa, F., Lee, S., Zalasiewicz, J., 2014. A refined foraminiferal biostratigraphy for the Late Campanian-Early Maastrichtian succession of northeast Iraq. GeoArabia, 19(1), 161-180.

Jain, S., Farouk, S., 2017. Shallow water agglutinated foraminiferal response to Late Cretaceous-Early Paleocene sea-level changes in the Dakhla Oasis Western Desert, Egypt, Cretaceous Research. 78, 240–257.

Jain, S., Niazi, M., Abdelhady, A. A., Vahidinia, M., Hossein, M. G. M., 2020. The Campanian paleoenvironment: inferences based on benthic foraminifera from northeastern Iran. palaeogeography, palaeoclimatology, palaeoecology, 554, 109823.

Jorissen, F.J., de Stigter, H.C., Widmark, G.V., 1995. A conceptual model explaining benthic foraminiferal microhabitats. Mar. Micropaleontol. 26, 3–16.

Jorissen, F.J., Fontanier, C., Thomas, E., 2007. Chapter seven paleoceanographical proxies based on deep-sea benthic foraminiferal assemblage characteristics. In: Hillaire-Marcel, C., De Vernal, A. (Eds.), Developments in Marine Geology, Proxies in Late Cenozoic Paleoceanography. Elsevier, pp. 263–325. https://doi.org/10.1016/ S1572-5480(07)01012-3.

Kaiho, K., 1991. Global changes of Paleogene aerobic/anaerobic benthic foraminifera and deep-sea circulation. Palaeogeogr. Palaeoclimatol. Palaeoecol. 83 (1-3), 65–85.

Kaiho, K., Hasegawa, T., 1994. End-Cenomanian benthic foraminiferal extinction and oceanic dysoxic events in the northwestern Pacific Ocean. Palaeogeography, Palaeoclimatology, Palaeoecology. 111, 29–43

Katz, M. E., Miller, K. G., Kaminski, M. A., Browning, J. V., 2018. Neogene benthic foraminiferal biofacies, paleobathymetry, and paleoenvironments of a Gulf of Mexico transect. Journal of Foraminiferal Research, 48(4), 356-372.

Keller, G., 1988a. Extinction, survivorship and evolution of planktic foraminifera across the Cretaceous/Tertiary boundary at El Kef, Tunisia: Marine Micropaleontology, 13, 239-263.

Keller, G., 1988b. Biotic turnover in benthic foraminifera across the Cretaceous/Tertiary boundary at El Kef, Tunisia: Palaeogeogr. Palaeoclimatol. Palaeoecol., 66, 153-171.

Keller, G., Adatte, T., Stinnesbeck, W., Affolter, M., Schilli, L., Lopez-Oliva, J.G., 2002. Multiple spherule layers in the Late Maastrichtian of northeastern Mexico, Geol. Soc. Am. 356, 145–162.

Khalil, H., Meshaly, S., 2004. Stratigraphy and stage boundaries of the Upper Cretaceous-Lower Paleogene succession in Gabal Musaba Salama area, southwestern Sinai, Egypt. Egyptian Journal Paleontology, 4, 1-38.

Klitsch, E., 1978. Geologische Bearberitung Südwest Agyptens. Geol. Rdsch., vol. 67, p. 507-520, Stuttgart.

Kouwenhoven TJ, Van der Zwaan GJ (2006) A reconstruction of late Miocene Mediterranean circulation patterns using benthic foraminifera. Palaeogeogr Palaeoclimatol Palaeoecol 238:373–385

Leckie, R.M., Olson, H.C., 2003. Foraminifera as proxies of sea level change on siliciclastic margins. SEPM Spec. Publ., 75.

Li, L., Keller, G., 1998a. Maastrichtian climate, productivity and faunal turnover in planktic foraminifera in south Atlantic DSDP Sites 525 A and 21. Marine Micropaleontology, 33, 5-86.

Li, L., Keller, G., 1998b. Abrupt deep-sea warming at the end of the Cretaceous. Geology. 26, 995-998.

Li, L.; Keller, G., Stinnesbeck, W., 1999. The late Campanian and Maastrichtian in northwestern Tunisia: paleoenvironmental inferences from lithology, macrofauna and benthic foraminifera. Cretaceous Research, 20, 231-252.

Lüger, P., 1985. Stratigraphie der marinen Oberkreide und des Alttertiärs im südwestlichen Obernil- Beeken (W-Ägypten) under besonderrer Berücksichtigung der Mikropaläontologie, Palökologie und Paläogeographie. Berliner Geowiss., Abh., A (63), 151 p., 22 fig., 11 tab., 24 pl., Berlin.

Lüning, S., Kolonic, S., Belhadj, E. M., Belhadj, Z., Cota, L., Barić, G., Wagner, T., 2004. Integrated depositional model for the Cenomanian-Turonian organic-rich strata in North Africa. Earth-Science Reviews, 64(1-2), 51-117.

M.H. El-Dawy, Paleocene benthic foraminiferal biostratigraphy and paleobathymetry in the sections between El Sheikh Fadl and Ras Gharib Eastern Desert, Egypt, Micropaleontol. Micropaleontol. 47 (1) (2001) 23–46.

Metwally, A. A., Mohamed, A. A., Obaidalla, N. A., Salman, A. M., Mahfouz, K. H., 2023. Cretaceous–Paleogene (K–Pg) boundary in south Sinai, Egypt: Paleoenvironment and sequence stratigraphy implications. Journal of African Earth Sciences, 205, 105017.

Miller, K.G., Browning, J.V., Aubry, M.-P., Wade, B.S., Katz, M.E., Kulpecz, A.A., Wright, J.D., 2008. Eocene-Oligocene global climate and sea-level changes: St Stephens Quarry, Alabama, Geol. Soc. Am. Bull. 120 (1–2), 34–53.

Miller, K.G., Schmelz, W.J., Browning, J.V., Kopp, R.E., Mountain, G.S., Wright, J.D., 2020. Ancient sea level: as key to the future. Oceanography 33, 32–41.

Miller, Kenneth G., Michelle A. Kominz, James V. Browning, James D. Wright, Gregory S. Mountain, Miriam E. Katz, Peter J. Sugarman, Benjamin S. Cramer, Nicholas Christie-Blick, and Stephen F. Pekar. "The Phanerozoic record of global sea-level change." *science* 310, no. 5752 (2005): 1293-1298.

Murray, J. W., 2006. Ecology and applications of benthic foraminifera. Cambridge University Press.

Murray, J. W., Alve, E., 2011. The distribution of agglutinated foraminifera in NW European seas: Baseline data for the interpretation of fossil assemblages. Palaeontologia Electronica, 14(2), 1-41

Murray, J.W., 2000. When Does Environmental Variability Become Environmental Change? The Proxy Record of Benthic Foraminifera. In: Environmental Micropaleontology: The Application of Microfossils to Environmental Geology, Topics in Geobiology, 15, Martin, R.E. (Ed.). Plenum Press, New York, 7-37.

Nouradini, M., Azami, S.H., Hamad, M., Yazdi, M., Ashouri, A.R., 2015. Foraminiferal paleoecology and paleoenvironmental reconstructions of the lower Miocene deposits of the Qom Formation in Northeastern Isfahan, Central Iran Boletín Soc. Geol. Mexicana 67 (1), 59–73.

O'Brien, C.L., Robinson, S.A., Pancost, R.D., Sinninghe Damst´e, J.S., Schouten, S., Lunt, D.J., Alsenz, H., Bornemann, A., Bottini, C., Brassell, S.C., Farnsworth, A., Forster, A., Huber, B.T., Inglis, G.N., Jenkyns, H.C., Linnert, C., Littler, K., Markwick, P., McAnena, A., Mutterlose, J., Naafs, B.D.A., Püttmann, W., Sluijs, A., van Helmond, N.A.G.M., Vellekoop, J., Wagner, T., Wrobel, N.E., 2017. Cretaceous sea-surface temperature evolution: constraints from TEX86 and planktonic foraminiferal oxygen isotopes. Earth Sci. Rev. 172, 224–247. https://doi.org/10.1016/j.earscirev.2017.07.012

Olsson, R.K. and Nyong, E.E., 1984. A paleoslope model for Campanian-lower Maestrichtian foraminifera of New Jersey and Delaware. *The Journal of Foraminiferal Research*, *14*(1), pp.50-68.

Orabi, O. H., Zahran, E., 2014. Paleotemperatures and paleodepths of the upper cretaceous rocks in El Qusaima, northeastern Sinai, Egypt. Journal of African Earth Sciences, 91, 79-88.

Ortakand, M. S., Hasegawa, S., Matsumoto, R., 2015. Biostratigraphic and palaeoecologic evaluation of the Japan Sea's Joetsu Basin based on the study of foraminifera. Paleontological Research, 19(2), 79-106.

Ott d'Estevou, P., Bolze, J., Montenat, C., 1986. Etude geoloique de la marge occidentale du Golfe de Suez : le massif des Gharamul et le Gebel Dara. Documents et Travaux. Inst. Geol. Albert de Lapparent (IGAL), 10, 19-43, Paris.

Permian, A., 2013. III. Geologic History. The Tethys Ocean, 8, 246.

Rahmouna, J., Barhoun, N., Rachid, A., Targhi, S., Bahaj, H., Berry, N., & Yousfi, M. Z. (Year). Late Miocene–Early Pliocene paleoenvironmental changes in the western Rifian corridor (NW Morocco). *Environmental Earth Sciences (2022) 81:528 https://doi.org/10.1007/s12665-022-10648-7*

Robaszynski,F., Caron,M., Gonzalez Donoso,J.M.,Wonders, A.A.H. Atlas of Late Cretaceous Globotruncanids, Rev. Micropaleont. 26 (1984) 145–305.

Rosenberg, Y. O., Ashckenazi-Polivoda, S., Abramovich, S., Thibault, N., Chin, S., Feinstein, S., ... Amrani, A., 2021. Resilience of primary and export productivity in a eutrophic ecosystem following the Cretaceous-Paleogene mass extinction. Global and Planetary Change, 196, 103371

Said, R., 1960. Planktonic foraminifera from the Thebes Formation, Luxor. Micropal., vol. 6, p. 277-286.

Said, R., 1961. Tectonic framework of Egypt and its influence on distribution of foraminifera. Bull. Amer. Assoc. Petrol. Geol., 45, 198–218.

Said, R., 1962. The Geology of Egypt. Elsevier Publication Co., Amsterdam New-York, 377p.

Saidi, E., Zaghbib-Turki, D., 2016. Planktonic foraminiferal biostratigraphy and quantitative analysis during the Campanian-Maastrichtian transition at the Oued Necham section (Kalâat Senan, central Tunisia). Turkish Journal of Earth Sciences, 25(6), 538-572.

Saint-Marc, P., 1992. Biogeographic and bathymetric distribution of benthic foraminifera in Paleocene El Haria Formation of Tunisia. *Journal of African Earth Sciences (and the Middle East)*, *15*(3-4), pp.473-487.

Sakai, K., Ohkushi, K. I., Shibahara, A., 2021. Biotic response of benthic foraminifera to OMZ variations in the northwestern Pacific since the last deglaciation. Geo-Marine Letters, 41(1), 5.

Saleh, S., Pamukçu, O., Brimich, L., 2017. The major tectonic boundaries of the Northern Red Sea rift, Egypt derived from geophysical data analysis. Contributions to Geophysics & Geodesy, 47(3), 149.

Scotese, C.R., 2014. Atlas of Late Cretaceous maps. In: PALEOMAP Atlas for ArcGIS, 2, pp. 16–22

Sen Gupta, B.K., and Machain-Castillo, M.L., 1993. Benthic foraminifera in oxygen-poor habitats. Mar. Micropaleontol. 20, 183–201.

Shahar, J., 1994. The Syrian arc system: An overview: Palaeogeography, Palaeoclimatology, Palaeoecology, 112, 125-142.

Shahin, A. M., 1988. Fossil fauna and stable isotopic composition within the Late Cretaceous- Early Tertiary at Gabal Nezzazat, Sinai, Egypt. Ph. D. Thesis, Mansoura Univ., Faculty of Science, Mansoura University, 212 pp.

Shirazi, B.G., Bakhshandeh, L., Yazdi, A., 2014. Biozonation and Paleobathymetry on Foraminifera Upper Cretaceous Deposits of Central Iran Basins (Isfahan, Baharestan Section), Open J. Geol. 4 (08), 343.

Soudry, D., Glenn, C.R., Nathan, Y., Segal, I., VonderHaar, D., 2006. Evolution of Tethyan phosphogenesis along the northern edges of the Arabian-African shield during the Cretaceous-Eocene as deduced from temporal variations of Ca and Nd isotopes and rates of P accumulation. Earth-Science Reviews, 78(1-2): 27-57.

Speijer, R. P., Van der Zwaan, G. J., 1994. The differential effect of the Paleocene/Eocene boundary event: extinction and survivorship in shallow to deep-water Egyptian benthic foraminiferal assemblages. In: R. P. Speijer, Extinction and Recovery Pattern in Benthic Foraminiferal Paleocommunities across the Cretaceous/Paleogene and Paleocene/Eocene Boundaries. Ph. D. Thesis, Utrecht Univ. Geol. Ultraiect., 124, 121-168.

Speijer, R.P., Schmitz, B., 1998. A benthic foraminiferal record of Paleocene sea level and trophic/redox conditions at Gebel Aweina, Egypt, Palaeogeogr. Palaeoclimatol. Palaeoecol. 137 (1-2), 79-101.

Sprong, J., Kouwenhoven, T., Bornemann, A., Dupuis, C., Speijer, R. P., Stassen, P., Steurbaut, E., 2013. In search of the Latest Danian Event in a paleobathymetric transect off Kasserine Island, north-central Tunisia, Palaeogeogr. Palaeoclimatol. Palaeoecol. 379, 1-16.

Székely, S.-F., Bindiu-Haitonic, R., Filipescu, S., Bercea, R. 2017. Biostratigraphy and paleoenvironmental reconstruction of the marine Lower Miocene Chechiș Formation in the Transylvanian Basin based on foraminiferal assemblages, Carnets Geol. 17 (2), 11.

Szinger, B., 2008. Early Cretaceous foraminifera from atoll environment (Márévár Valley, Mecsek Mountains, Hungary): 125th Anniversary of the Department of palaeontology at Budapest University. Jubilee volume of, Hantkeniana 6, 127-143.

Taha, S. A. A., Ali, M. Y., 2024. Benthic foraminiferal paleobathymetry and paleoenvironments of late Maastrichtian–early Eocene sequence in Wadi Tarfa, north Eastern Desert, Egypt. Egyptian Journal of Geology, 68(1), 289-307.

Tawadros, E. E., 2001. Geology of Egypt and Libya: Rotterdam, A. A. Balkema, 468 p.

Trubin, Y. S., Kamoun, M., Langer, M. R., 2023. Environmental Signatures Preserved in Extremely Shallow-Water Benthic Foraminiferal Assemblages from Oman, Arabian Sea. Journal of Foraminiferal Research, 53(4), 362-377.

Usami, K., Ohi, T., Hasegawa, S., Ikehara, K., 2013. Foraminiferal records of bottom-water oxygenation and surface-water productivity in the southern Japan Sea during 160–15 ka: associations with insolation changes. Marine Micropaleontology, 101, 10-27.

Van der Zwaan GJ, Jorissen FJ, Destigter HC (1990) The depth dependency of planktonic benthic foraminiferal ratios. Constraints and applications. Mar Geol 95:1–16

van der Zwaan, G.J., Duijnstee, I.A.P., den Dulk, M., Ernst, S.R., Jannink, N.T., Kouwenhoven, T.J., 1999. Benthic foraminifera: proxies or problems? A review of paleoecological concepts. Earth-Sci. Rev. 46, 213–236.

Van Hinsbergen DJJ, Kouwenhoven TJ, van der Zwaan GJ (2005) Paleobathymetry in the backstripping procedure: correction for oxygenation effects on depth estimates. Palaeogeogr Palaeoclimatol Palaeoecol 221:245–265

Vancoppenolle, I., Vellekoop, J., Doubrawa, M., Kaskes, P., Sinnesael, M., Jagt, J. W., ... Speijer, R. P., 2022. The benthic foraminiferal response to the mid-Maastrichtian event in the NW-European chalk sea of the Maastrichtian type area. Netherlands Journal of Geosciences, 101, e12.

Wang, D., Gouhier, T. C., Menge, B. A., Ganguly, A. R., 2015. Intensification and spatial homogenization of coastal upwelling under climate change. Nature, 518(7539), 390-394.

Youssef, M. M., 2003. Structural setting of central and south Egypt: an overview. Micropaleontology, 49 (Suppl_1), 1-13.

Youssef, M., 1957. Upper Cretaceous rocks in Kosseir area. Bull. Inst. Desert Egypt, 7, No. 2, 35-53, Cairo.